Copper Heat Sink Design

A Practical Application of Mathematical Modelling

By

Jafar Mahmoudi* and Jussi Vaarno+

* Outokumpu Fabrication Technologies, R&D, Västerås, Sweden, jafar.Mahmoudi@outokumpu.com
+ Outokumpu Research Center, Pori, Finland, Jussi.Vaarno@outokumpu.com

Abstract

In this work, a new concept for cooling the electronic components using the copper-base heat sink is proposed. The thermal performance and temperature distribution for the heat sink were analysed and a procedure for optimising the geometrical design parameter is presented. A three-dimensional model is developed to investigate flow and conjugate heat transfer in the copper-based heat sink. The model was produced with the commercial program FLUENT. The theoretical model developed is validated by comparing the predictions of the model with available experimental data.
Several examples with different types of cooling methods and manufacturing processes are analysed to show the reliability and effectiveness in heat spreading of those. This report will also describe a modelling methodology that can be used to predict performance, with comparison to experimental data. The reliability of the presented model in optimising the copper-base heat sink design will be discussed.

Nomenclature

w: width [m] g: refer to air
l: length [m]
d: height [m]
t: thickness [m]
η_f: fin efficiency
p: pressure [pa]
Q, q: heat flux [W, W/m^2]
h: heat transfer coefficient [W/m^{2}K]
Re: Reynolds number, $\rho uD/\mu$
T: temperature [K]
u,v,w: velocity components [m/s]
μ: Dynamic viscosity [N/sm^2]
ρ: density [kg/m^3]
k: effective thermal conductivity [W/mK]
C_p: Thermal capacity [J/kgK]
P, ΔP: Pressure and Pressure drop [N/m^2, Pa]
$\dot{m}$: mass flow rate [kg/s]
b: refer to air
i: refer to input
w: refer to wall/solid
o: refer to inlet

Keywords: *Heat sink designn* conjugate boundary condition*, mathematical modelling, fluid flow, heat transfer*

1. Introduction

The heat removal problem has become an important factor in the advancement of microelectronics due to both drastically increased integration density of chips in digital devices as well as an increased current density capability of power electronic devices. The task of removing a large amount of dispersed heat from a constrained, small space is often beyond the capability of conventional cooling techniques, therefore, new methods with removal capabilities at least one order larger than that of conventional ones are required [1-5].
Increasing the power dissipation and mounting density of electronic equipment are requiring more effective thermal systems to cool the chip and device. One the commonly used method for the effective thermal enhancement is to use heat sinks [6-9].
The undesirable temperature gradient is an important consideration in the design of an electronic cooling scheme. A large temperature rise produces thermal stresses in chips and packages due to the coefficient of thermal expansion (CTE) mismatch among different materials; thus undermining device reliability [10-17]
Sabry [18] proposed a mechanism for heat transfer improvement based on the increased importance of surface roughness for small channels. The relation deduced for fluid flow perfectly matched friction data. As for heat transfer, the proposed relation was closer to measured *h* than standard correlations, but still predicting higher values. It was concluded that another mechanism might have contributed to heat transfer reduction.
In this work, a thermal design and evaluation method for heat sink is presented. The thermal performance of the proposed Al-base heat sink is examined numerically using a finite volume method. The optimisation issues for design parameters for a new copper base heat sink are addressed as well.

2. Modelling

2.1 Theoretical approach

The dissipated heat from an electronic device is transferred to a heat sink through case and gap material. Subsequently this heat is transferred from the heat sink to ambient air. It is ultimate aim to design heat sink geometry so that estimated junction temperature of heat sink should be no greater than prescribed junction temperature.
The successful design of the copper heat sink requires fundamental understanding of the transport methods during cooling process. Detailed measurements and predictions of the local temperature and heat fluxes are critically important for development of the compact, efficient, and reliable systems for thermal management. In this paper, we employ the numerical simulations to gain insight into combined convection-conduction heat transfer in different rectangular and circular unit cell of the electronic heat sink. To this end, a system of three-dimensional Navier-Stokes equations for conservation of mass, momentum and energy based on the continum flow assumption is used as a mathematical model of the process.

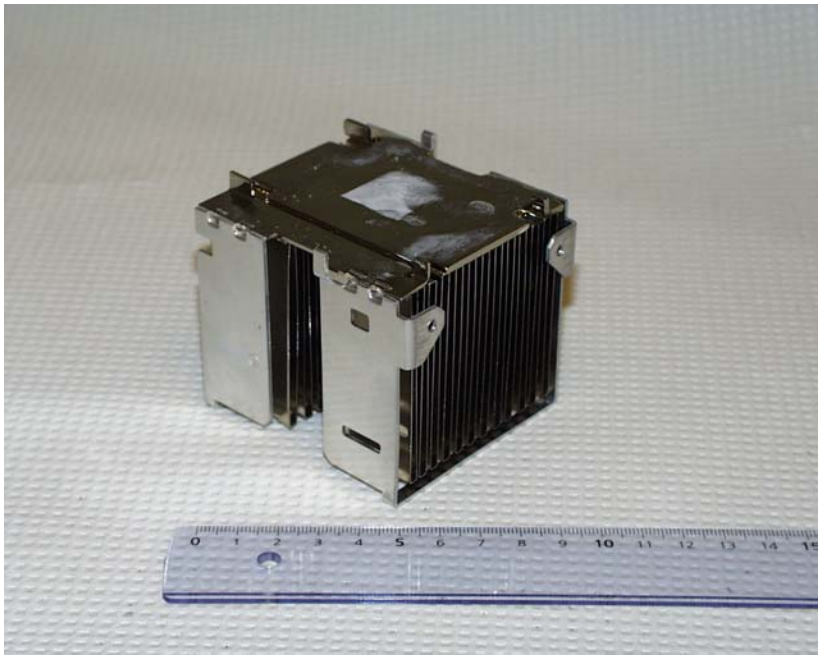

Fig.1) Al-base heat sink

Consider a three-dimensional rectangular heat sink studied in this work. The air with uniform velocity and the temperature T_1 is flowing through the heat sink unit. The temperature is increased to T_2. The heat, Q, transferred from the heat sink is:

$$Q = hA\left(T_{surface} - T_{air}\right) \tag{1}$$

which is absorbed by the air:

$$Q = \dot{m} C_p \left(T_2 - T_1\right) \tag{2}$$

The thermal resistance of the fin can be calculated as:

$$R_{fin} = \frac{1}{\eta_{f_{fin}} h_{fin} A_{fin}} \tag{3}$$

Where h_{fin} stands for heat transfer coefficient over the fin surface and η_{fin} stands for the fin efficiency expressed by:

$$\eta_{fin} = \frac{\tanh\left(ml\right)}{ml} \tag{4}$$

Parameter m can be defined as:

$$m = \sqrt{2h_{fin} \Big/ kt} \tag{5}$$

The thermal resistance of the base material is given by:

$$R_{base} = \frac{1}{h_{base} A_{base}} \tag{6}$$

The combined thermal resistance of fin and base material can be expressed by:

$$R_f = \frac{1}{\frac{1}{R_{fin}} + \frac{1}{R_{base}}} \quad (7)$$

R_f explains the conductive part of the thermal resistance in a heat sink. The convective contribution can be simplified as:

$$R_{flow} = \frac{1}{\dot{m} C_P} \quad (8)$$

One could consider the spreading resistance as well by definition:

$$R_{spd} = \frac{T_{surface} - T_{air}}{Q} \quad (9)$$

The contribution of the spreading resistance to the overall device temperature rise is significant if the footprint of a heat sink is much larger than the size of the heat source,

Considering this, the total thermal resistance of a heat sink can be defined:

$$R_T = R_f + R_{flow} + R_{spd} \quad (10)$$

The pressure loss in a heat sink is also a sum of the kinetic and viscous losses, which with a very high degree of simplification can be expressed by:

$$\Delta P_{tot} = \left(\sum \xi + f \frac{L}{D_h} \right) \frac{1}{2} \rho v^2 \quad (11)$$

where, f defines the friction factor and ξ can be simplified as a sum of kinetic loss coefficients. More details can be found elsewhere [19-22]

However, the flow field surrounding heat sink caused by fin geometry is very complicated and coupled with the temperature field so that the analytic solution is not obtained easily.

2.2 Computation method

A theoretical model for flow and conjugate heat transfer is developed. The conservation equations of mass, momentum and energy for the fluid and solid can be written as:

a) Conservation of mass (continuity)

$$\nabla\left(\rho \vec{V}\right) = 0 \quad (13)$$

b) Conservation of momentum

$$\vec{V}.\nabla\left(\rho \vec{V}\right) = -\nabla p + \nabla.\left(\mu \nabla \vec{V}\right) \quad (14)$$

c) Conservation of energy for fluid

$$\vec{V}.\nabla\left(\rho c_p T_g\right) = \nabla.\left(k_g \nabla T_g\right) \quad (15)$$

d) Conservation of energy for solid

$$\nabla\left(k_w \nabla T_w\right) = 0 \quad (16)$$

The governing mass, momentum and heat equations were solved by using the commercial program, FLUENT. The governing equations were discretised using a finite-volume formulation and solved using the SIMPLEC algorithm.
In the absence of well-established experimental data, a uniform total heat flux equal to 70 W is imposed as a boundary condition at the heated area. The inlet velocity around 2 m/s with room temperature of the air entering the heat sink is specified. This velocity can cause a pressure drop around 20 Pa (equal to 0.1 in-H20) in the heat sink case No. 1, as will be discussed later. Therefore, a constant pressure drop around 25 Pa has been chosen as inlet boundary condition. A no-slip boundary condition is imposed on the velocity components at the heat sink wall. Finally, the continuity of the temperature and heat flux is used as the conjugate boundary condition to couple the energy equations for the fluid and solid phases.

2.3 Objectives

The *first* objective of this project is to develop a mathematical model to investigate flow and conjugate heat transfer in the heat sink. The theoretical model needs to be validated.

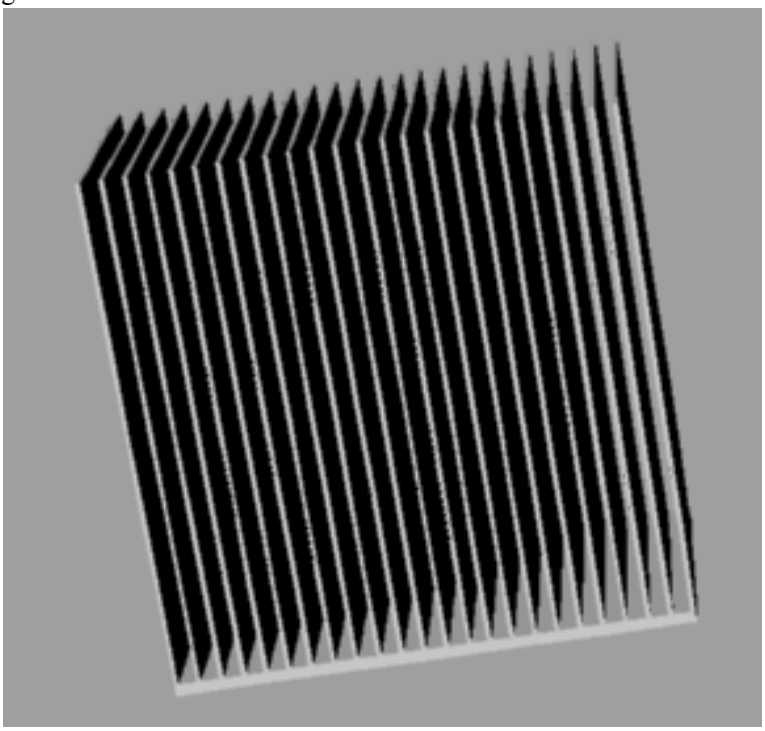

Fig.2a) Computational domain

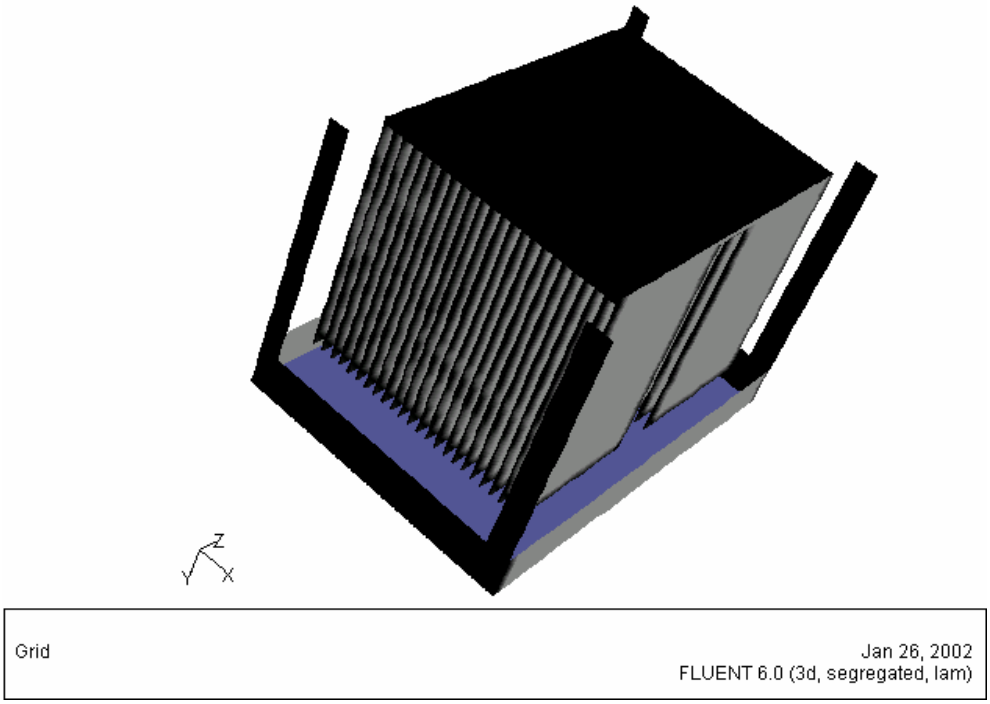

Fig.2b) Computational domain for case No. 1

This can be done by comparing the theoretical predictions of the model with available experimental data of different operational parameters in an Al-base heat sink, presented in Fig.1. The researched heat sink in this work is fabricated of extruded aluminium lamella plates (0.5 x 30 x 55) that are compressed together leaving 2 mm thick airflow ducts between the plates. The size of the heat sink is around 70 x 60 x 55 mm. The heat source is mounted to the base plate, which has thickness around 2 mm. The computational domain in this study is given in Fig.2.

Then, the local temperature, heat and mass flux will be analyzed with aim to identify the thermal performance established in three different possible unit cells of Cu-base heat sink, shown schematically in Fig. 3. The geometrical data for different cases are presented in Table 1.

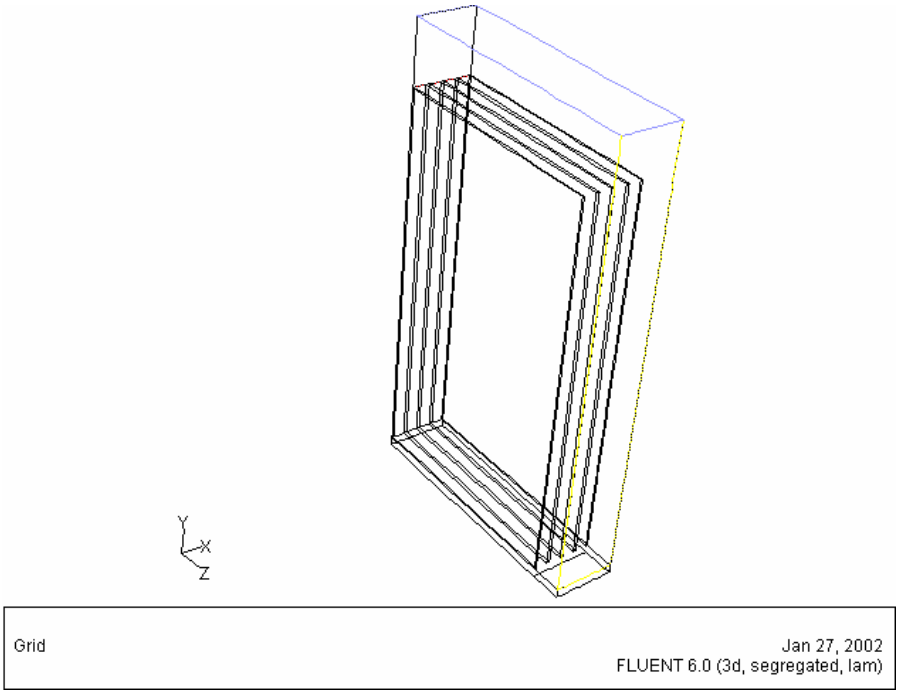

Fig. 3a) Unit cell for case No. 1

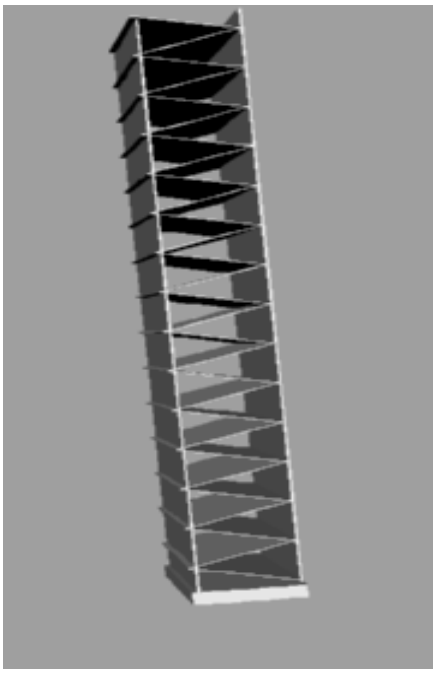

Fig. 3b) Unit cell for case No. 2

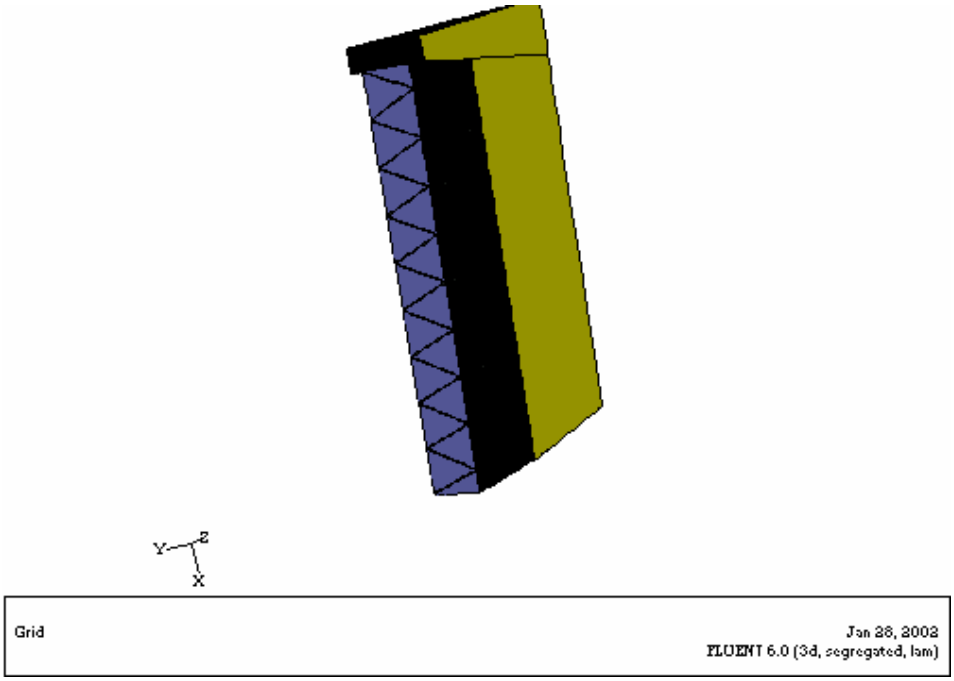

Fig. 3c) Unit cell for case No. 3

Table 1: geometrical data for different heat sink unit-cells

Case	**Dimension** *w x l x d (mm)*	**Fin** *t (mm), No*	**Support** *t (mm), No*	**Base-plate** *t (mm)*
Case No.1	10 x55x 35	0.5, 2	0.5, 2	2
Case No.2	10x55x35	0.1, 24	0.5 , 2	2
Case No.3	D=60, l=30, t=10	0.1, 24	0.5, 2	10

Case No.1: Rectangular heat sink based on straight fins
Case No.2: Rectangular heat sink based on triangle fins
Case No.3: Cylindrical heat sink based on triangle fins

Finally, the results will be used to evaluate four different possible construction designs for Cu-base heat sinks, schematically given in Fig. 4. The average heat transfer characteristics will be studied, and practical recommendations will be provided regarding the overall heat sink performance. The geometrical data for those cases are presented in Table 2.

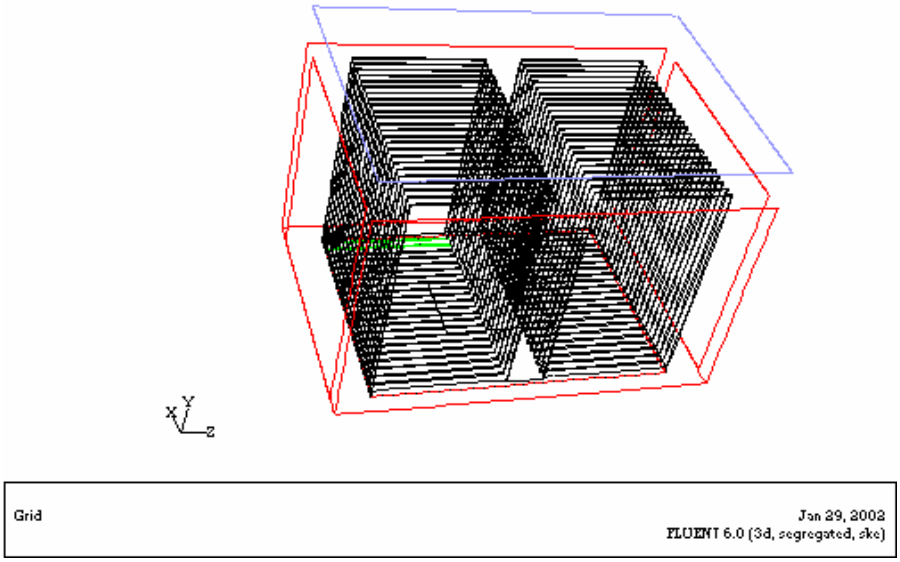

Fig. 4a) Computational domain for case No.1

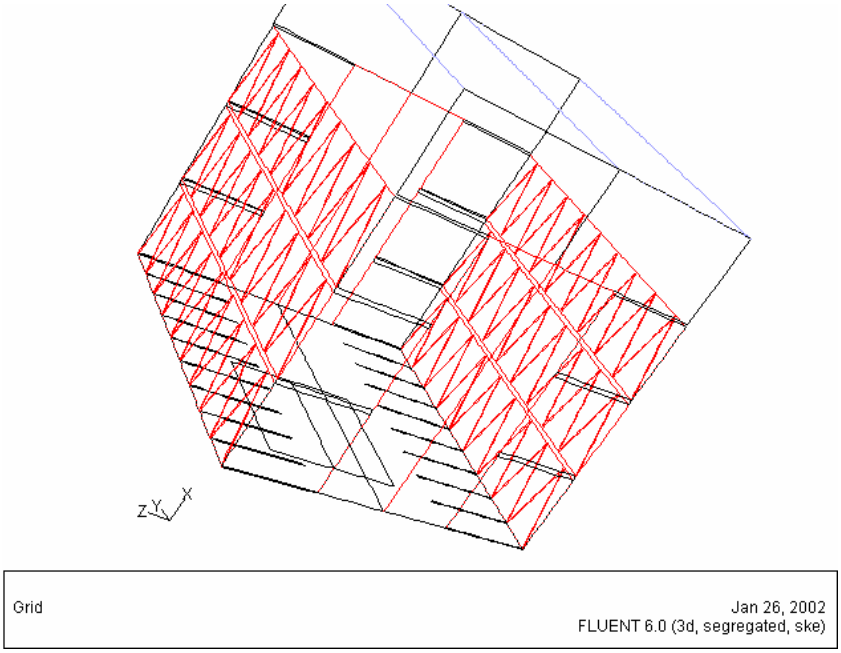

Fig. 4b) Computational domain for case No.2

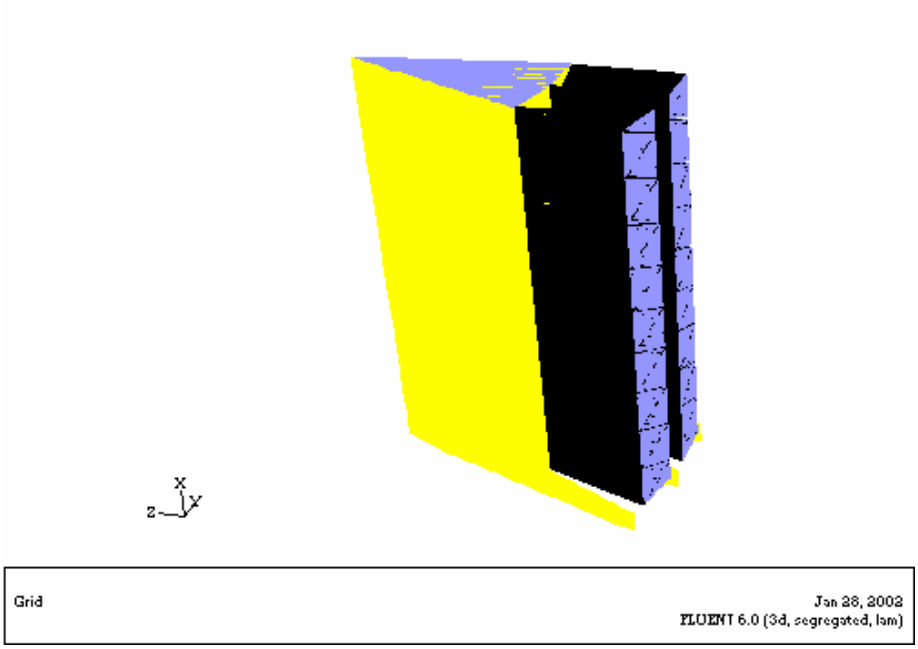

Fig. 4c) Computational domain for case No.3

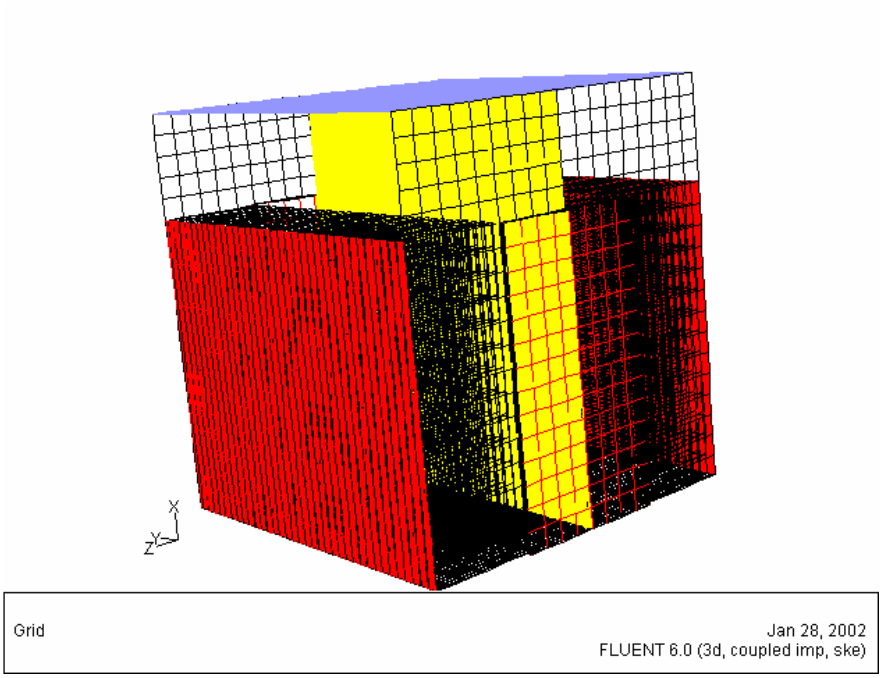

Fig. 4d) Computational domain for case No.4

Table 2: geometrical data for different heat sink

Case	Dimension *w x l x d (mm)*	Fin *t (mm), No*	Support *T (mm), No*	Calculated weight (g)
Case No.1	30x25x40	0.25, 24x2	0.5, 2x2	97
Case No.2	35x35x30	0.1, 24x12	0.5 , 6x2	76
Case No.3	D=60, l=30, t=10	0.1, 24 x21	0.5, 21	116
Case No.4	35x35x30	0.1, 35x2	0.5, 2x2	66

Case No.1: Rectangular heat sink based on straight fins
Case No. 2: Rectangular heat sink based on triangle fins
Case No.3: Cylindrical heat sink based on triangle fins
Case No. 4: Rectangular heat sink based on straight thin fins
Note: the calculated weight is obtained numerically based on the sum of the solid volume in each case, in which need to be more carefully evaluated.

2.4 Dimensionality

It was found that a three-dimensional model is necessary in this work, because the flow and consequently temperature distribution in the, specially, triangle base fin structure (cases 2 and 4) is expected to be three dimensional, along with a non-linear distribution in a stream wise direction. This will be discussed latter.

3. Experimental data

The following experimental data, have been used for boundary condition indata:

- Power: 76 W
- Allowable size of heat dissipation device: 88.9x 68.31x 60 mm
- Characteristic fan behaviour: 70x15mm with 39CFM air flow rate and 0.218 in H2O static pressure on CPU cooling device.

In order to evaluate the validity of the developed mathematical model the following measured data has been used:

- Allowable case temperature on CPU surface: 64 C

4. Analysis

The three-dimensional computation domain based on case number 1 (Al-base heat sink) has been earlier illustrated in Fig. 1. A uniform heat flux, *Q=70 W*, is applied on the 20 x 20 mm surface mounted at the centre of the bottom-plate of the heat sink. The thermal resistance between the heat source and the heat sink assumed to be negligible at this stage. The intaken fan of the correct size and power is applied on top of the heat sink. The air coolant is assumed to enter the heat sink from the top surface at a constant temperature. The fan is characterized by the Flow rate *vs* pressure drop, presented in Fig. 5. Obviously, the temperature variation associated with the air flow is dependent upon the pressure resistance in the heat sink, with a 0.1 *In.H20* or 24.5 *Pa* pressure drop produces around 11 CFM flow rate or around 4.2 m/s.
The numerical algorithm and the computer program were evaluated by comparing model predictions with available experimental data.

4.1 Al-base heat sink

It has been assumed that the heat sink was manufactured by compressing extruded aluminum plates with a thermal conductivity around 220 W/mK. The bottom plate of the heat sink has been treated as a homogenous material and the thermal resistance between the heat source and the bottom plate has been ignored. Further, the effect of the edge surfaces of the heat sink is ignored and the heat source is assumed to be generating uniform heat flux. Note that the heat source is centrally mounted on the bottom plate, and the heat sink is cooled uniformly over the exposed finned surface. In this calculations, it is assumed that all heating power is conducted to the fins so that external heat loses are negligible. The contribution of radiation is also neglected since the temperature difference is rather small. The relatively low absolute temperature has more influence on convective/radiative heat transfer is this case than temperature difference
The Reynold number for the flow rate in the heat sink channel shows that the laminar flow can be applied, even though the taken fan provides turbulent flow. However, the computation has been tested for both laminar and viscous turbulent flow. It found that no significant difference could be expected based on that.

Heat Source: 11 x 9 mm
Heat Dissipation: 45 W

Fan: 60 x 60 x 10 mm
Max- Air Flow Rate: 21.19 CFM
Max. Static Pressure: 0.169 mm.H2O

Ambient Temp: 35 C

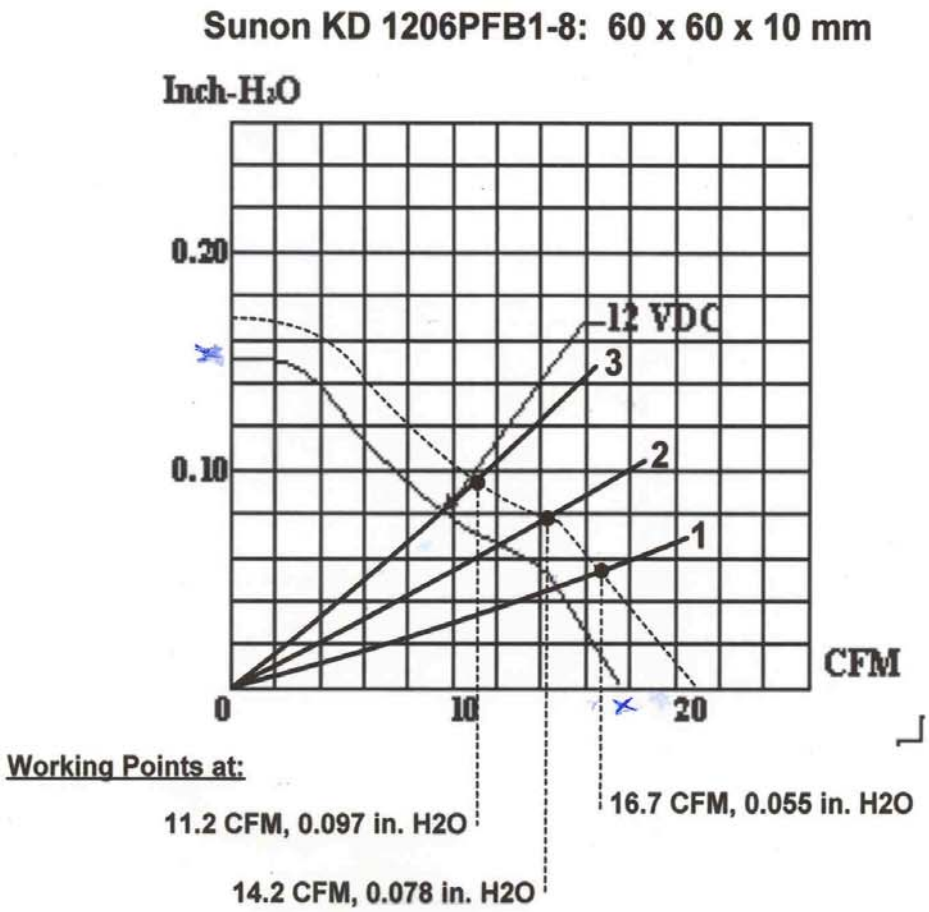

Fig. 5) Fan specificarion (Flow rate *vs* pressure drop)

Fig. 6 shows the shaded temperature contour plots in the Al-base heat sink. The temperature varies between 300 to 347 K at the heat source. It can be concluded that the

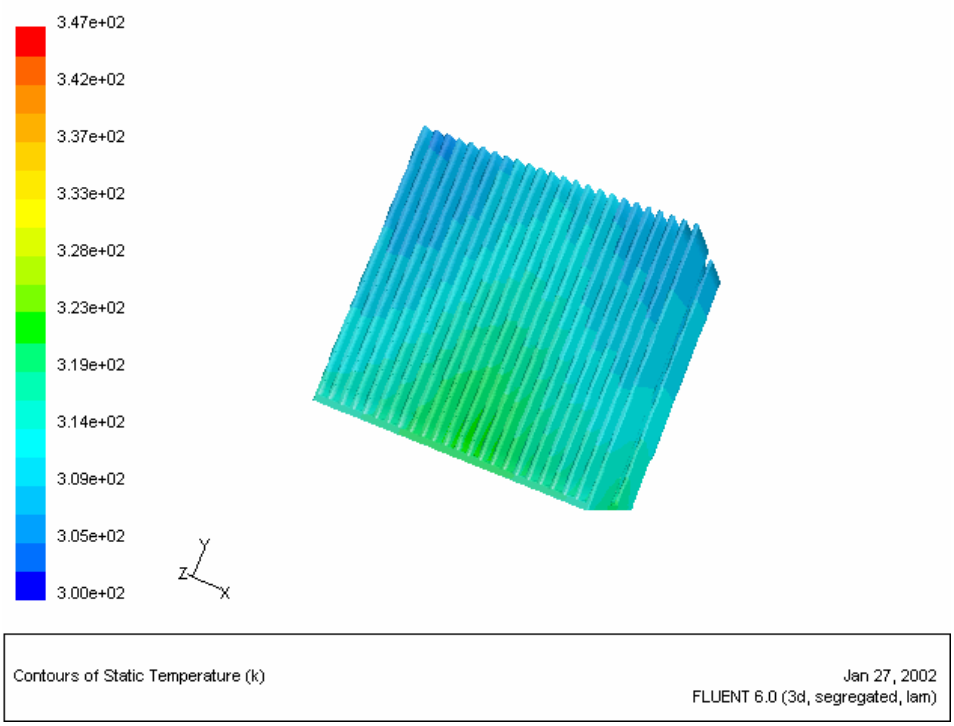

Fig. 6a) Temperature distribution in the fins

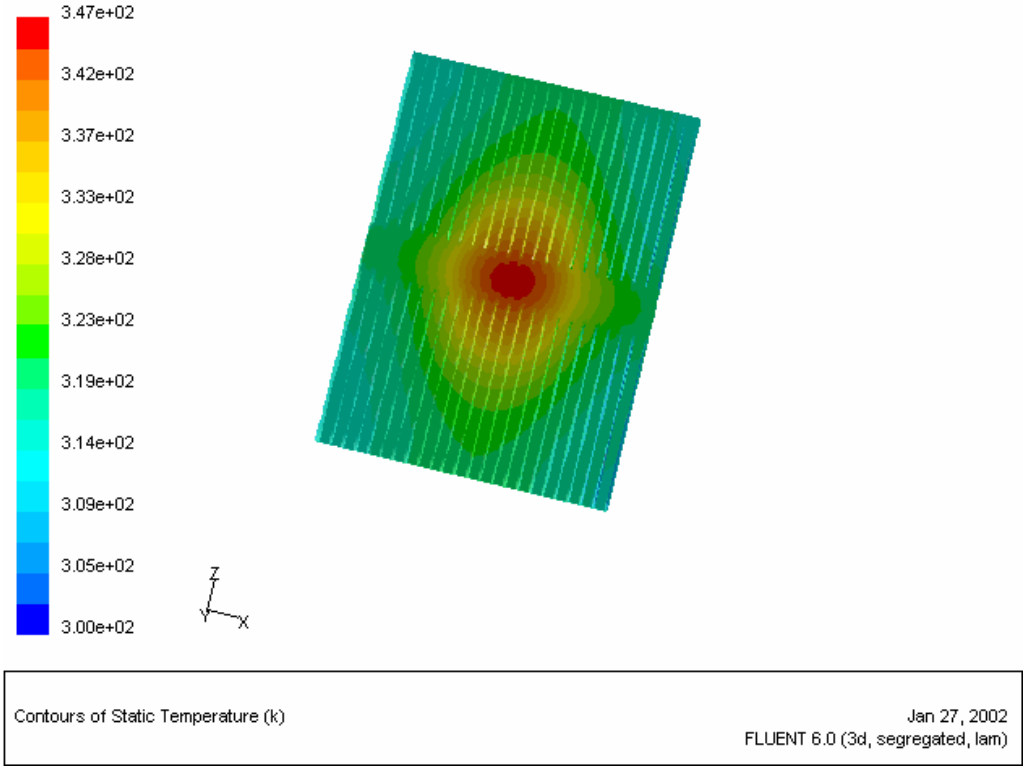

Fig. 6b) Temperature distribution in the bottom plate

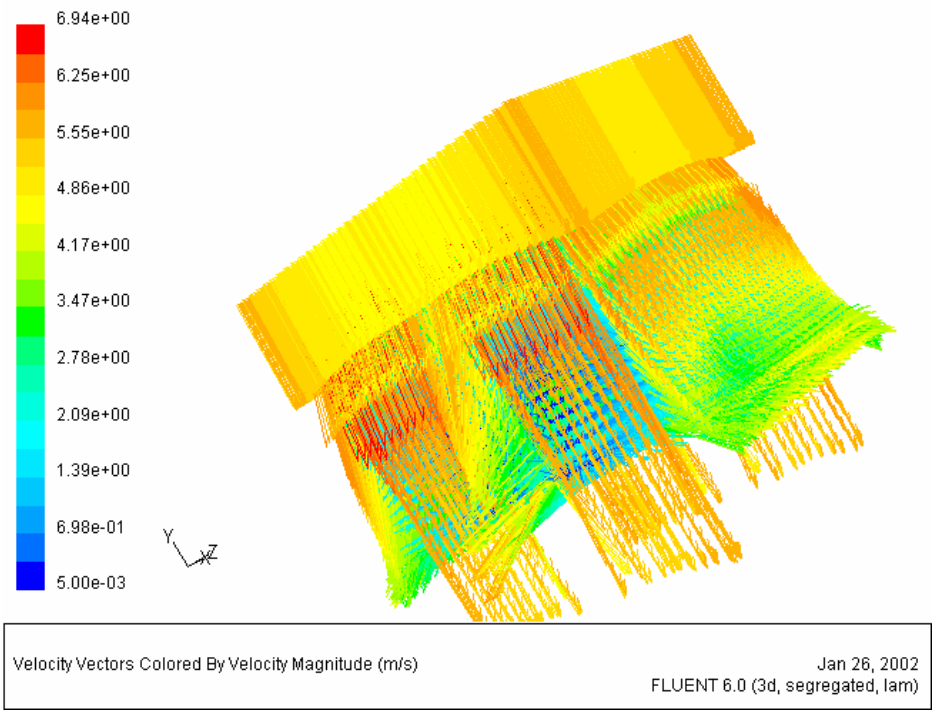

Fig. 7a) Velocity distribution in the domain

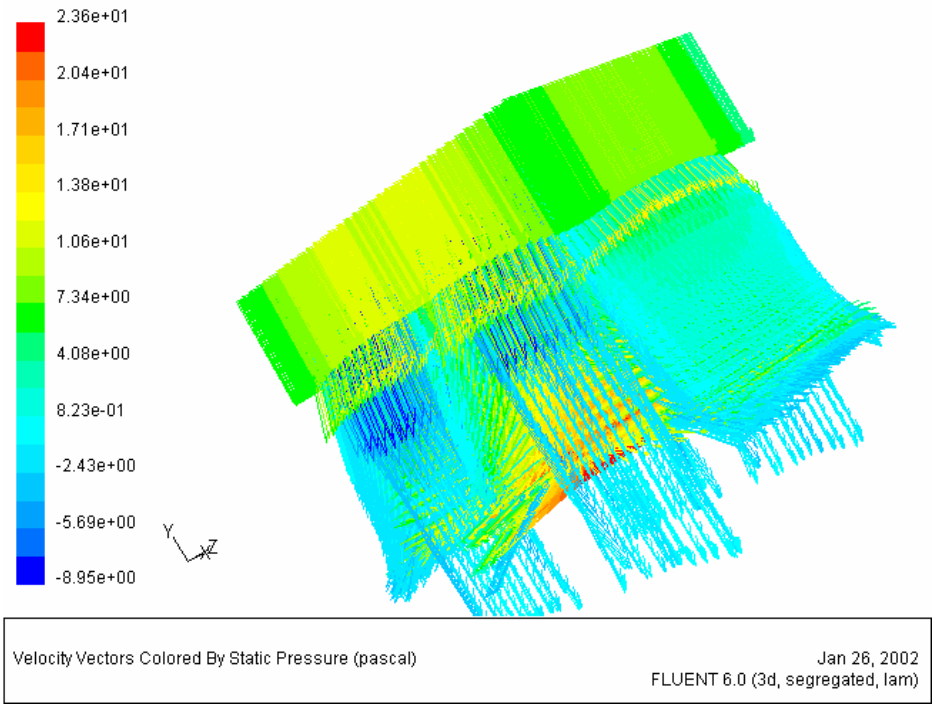

Fig. 7b) Pressure distribution in the domain.

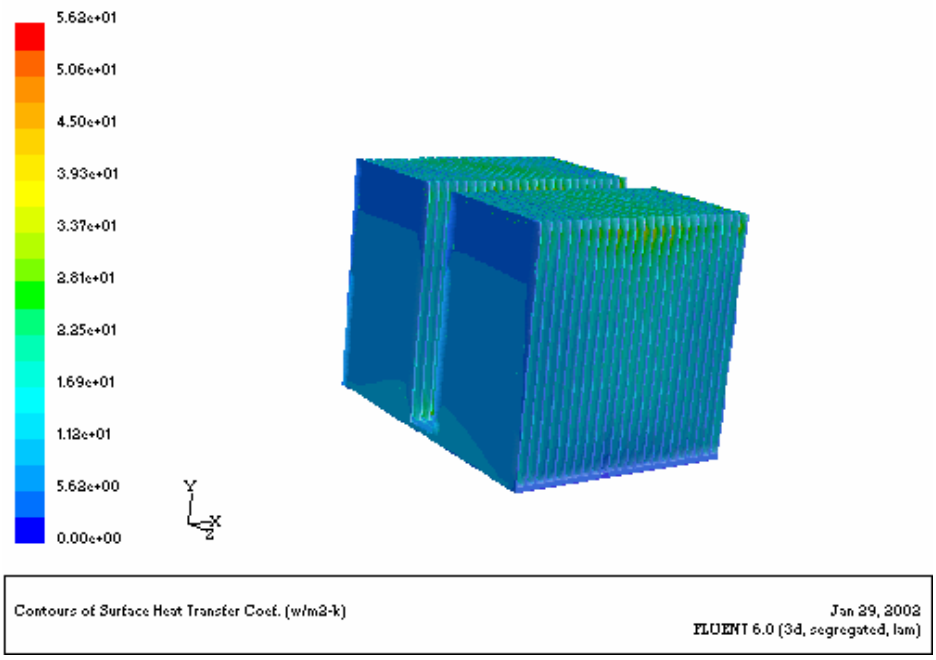

Fig. 8) Overall heat transfer coefficient

Prediction of the thermal parameters from simulations are within acceptable limit compared to those reported earlier.
Figs. 7(a,b) show the velocity and pressure distributions in the Al-base heat sink. The pressure drop in the system can be measured by comparing the inlet pressure with the ambient one. In this case a pressure drop around 24 Pa will cause for an average inlet velocity of 4.4 m/s, while a total mass flow around 0.037 kg/s will be provided by the fan. The mass flow rate at the inlet surface will be around 0.1617 (m/s)(kg/s). This looks again to be in the acceptable range of variation. Note that the pressure loss caused by the heat sink is an important factor when actual design is made.
The overall heat transfer coefficient, h, is presented in Fig. 8. It can be seen that the average value of h varies between 56 W/m^{2}K (at the fins) and 229 W/m^{2}K at the heat source surfaces. The results will be discussed in details shortly.

To this end (and in absence of more detailed experimental data) the validity of the present model has been studied by comparing the predicted results with available measured data; keeping in mind that more experiments will be desirable in this manner, providing the fact that, the model can be used for thermal design and evaluation technique for a Cu-base heat sink. The optimisation issues for design parameter will be addressed in next section.

4.2 Cu-base heat sink

In order to evaluate the functionality of the copper-base heat sink, the model has been used to numerically examine the performance of this new concept. The flow, temperature and pressure distributions for this new concept has been analysed and the procedure for optimising the geometrical design parameters has been studied based on the following considerations:

- lower cost
- less space occupation
- better technology
- and of course, made from copper

The results could be employed to evaluate if the copper-base heat sink is a substantial improvement over the conventional aluminium heat sink.

4.2.1 Copper in reference geometry

Let's consider replacing aluminium with copper in the three-dimensional rectangular symmetric heat sink presented earlier (Fig. 5-8). The results are given in Figs. 9-14 to illustrate the distributions of temperature, velocity, pressure and finally heat transfer coefficient respectively.

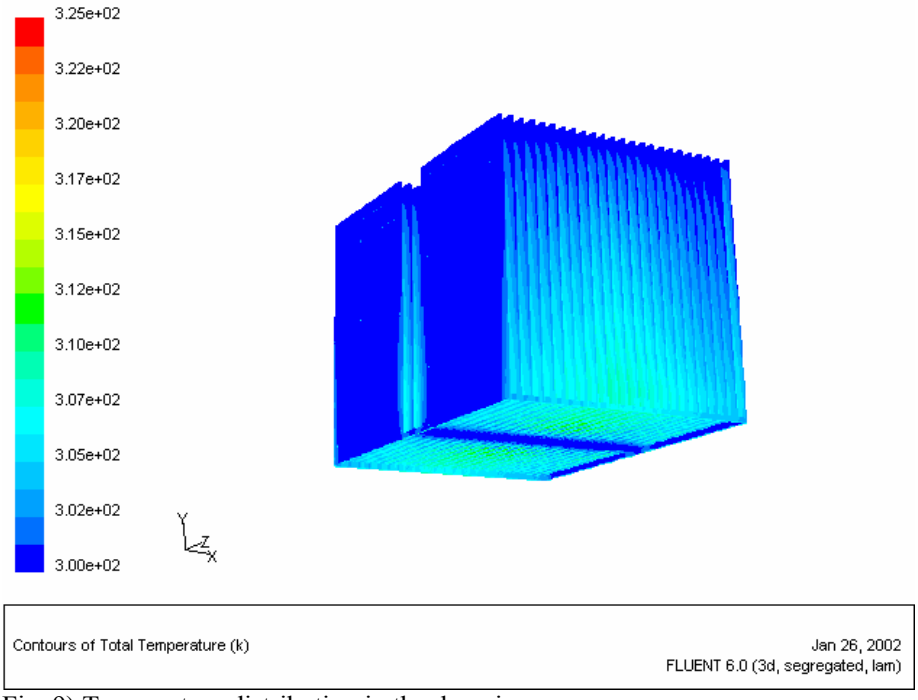

Fig. 9) Temperature distribution in the domain

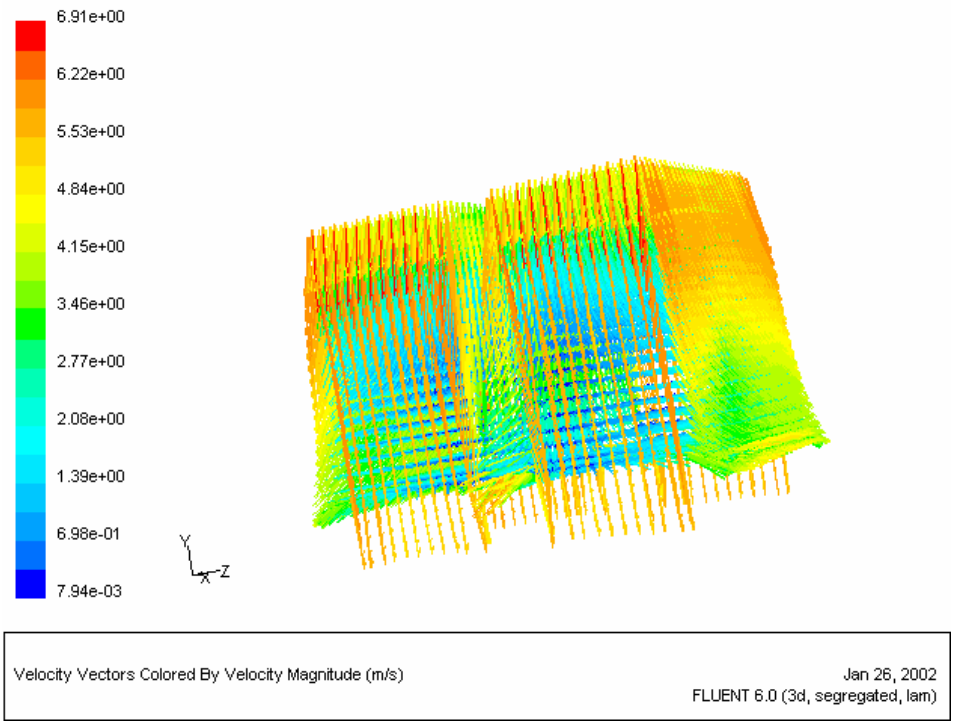

Fig.10) Velocity distribution in the domain

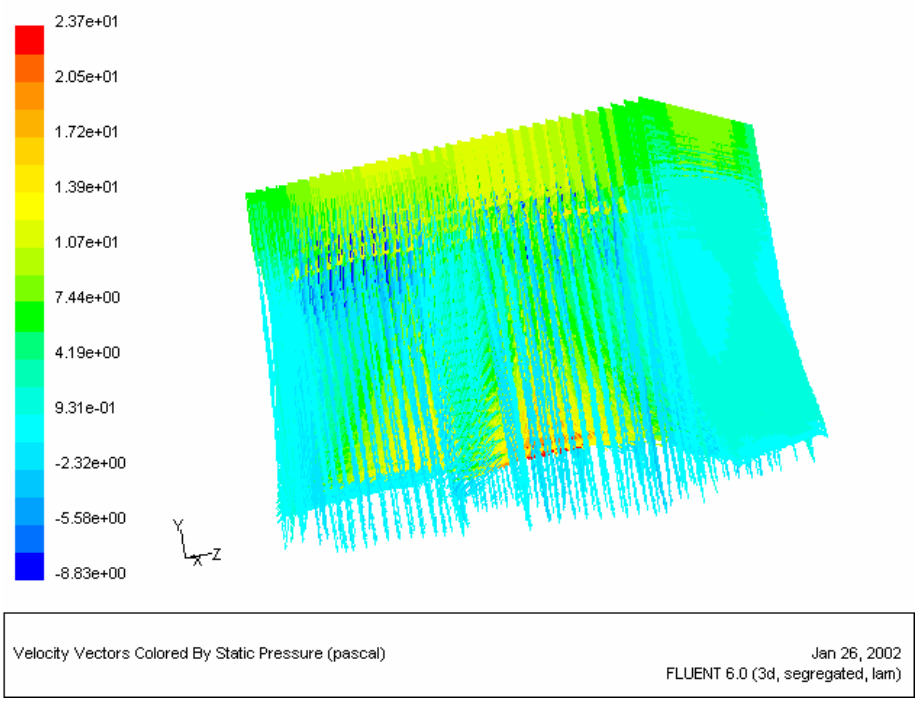

Fig.11) Pressure distribution in the domain.

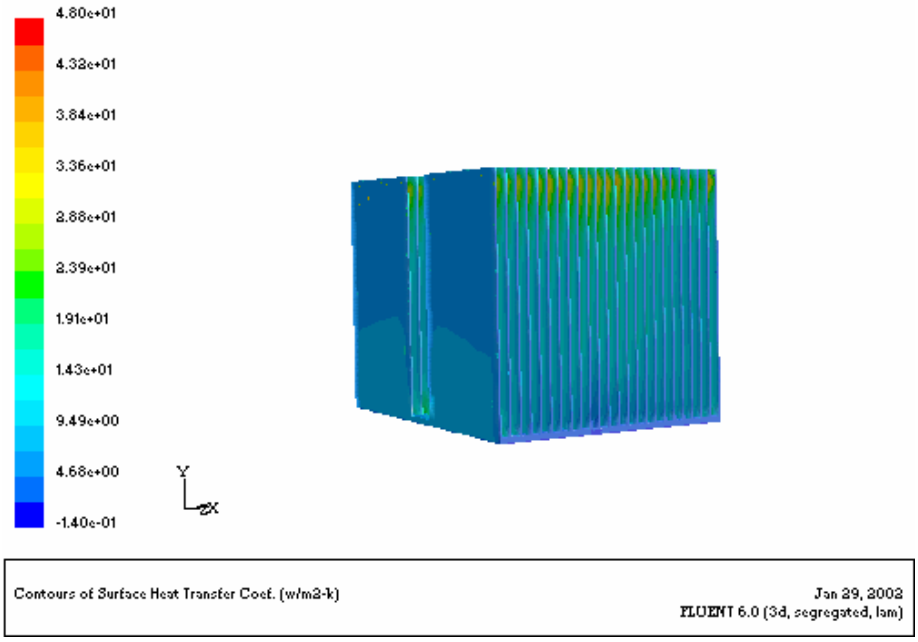

Fig.12) Overall heat transfer coefficient

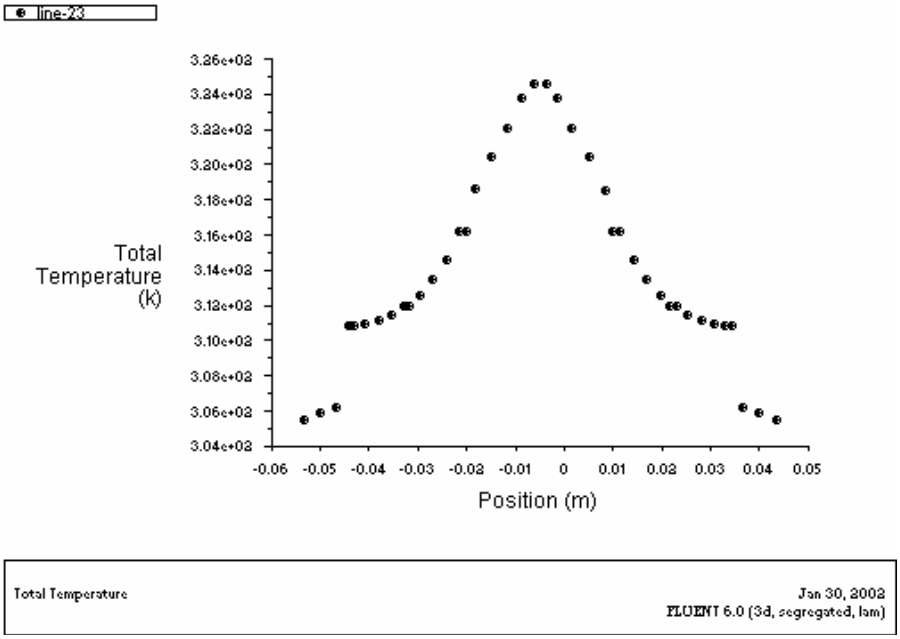

Fig.13) Temperature distribution in the bottom plate of the domain

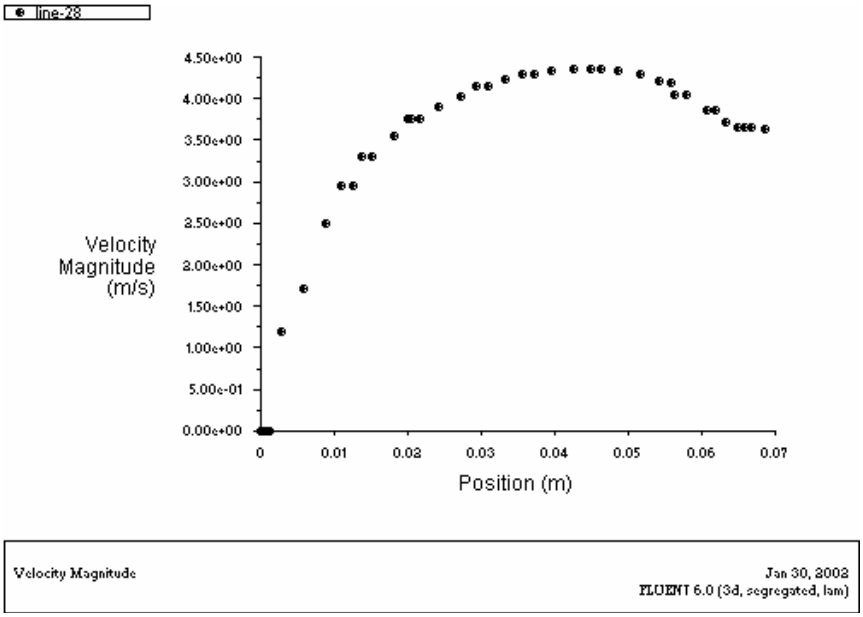

Fig.14) Velocity magnitude in the longitude direction

Fig. 9 together with Fig. 13 show the temperature distribution in a copper heat sink, applying same reference geometry and operating data, similar to those for aluminium case. It can be found that the maximum temperature for copper case is around 22 degree less than the aluminum one with a maximum temperature around 325 K. Note also that the heat spreads out faster in all x, y and z direction for copper case. This can be explained as follows:

Heat supplied at the fin base heat sink is conveyed along fins where it is gradually dissipated from the fin/fluid interface. This creates the well-known negative temperature gradient in longitudinal direction of the fins. Cooling air is forced to flow in the transverse direction. The close analysis of the thermal field evaluation indicates that the isotherms are closely packed everywhere, and gradually spread out within a simultaneous increase in the air region temperature. The air temperature at the outlet may be significantly higher than at the inlet. The

final part of the fins area will thus perform less heat dissipation than the starting part. The results indicate that:

- The intensity of heat transfer between solid and air is in its peak near the heat source at the bottom plate;
- The heat flux, imposed by the heat source, is immediately spread out by conduction within the bottom substrate and eventually is transferred to the air almost uniformly through all fins. The thermal development region does not occupy essentially the entire length of the fins owing to the conjugate convection-conduction interaction, which can be a positive sign for smaller heat sink at least in z-direction and in more conductive material like copper.

Figs. 10 shows the overall velocity distributions in the Al-base heat sink, when Fig. 14 depicts the spatial velocity distribution along the longitudinal direction. The velocity varies along y-axis from almost 7.9 e-3 to 6.9 m/s with the highest value at the top. The average inlet velocity, mass flux and mass flow rate at the inlet surface are around 4.4 m/s, 0.037 kg/s and 0.1616 (m/s)(kg/s) respectively.

The overall heat transfer coefficient, *h*, has been presented in Fig. 12. It can be seen that $\bar{h}$ varies between 49 W/m^{2}K (at the fins) to the highest 3605 W/m^{2}K (compare with 229 W/m^{2}K for aluminum) at the heat source surfaces. The results indicate that the cooling process is mainly controlled by conduction rather than convection for this geometry. That can be explained by existing a huge amount of copper, available for cooling process and remembering the fact that copper is a great material for conduction, which means it can pull off the heat from CPU faster than aluminum.

All together, indicates that a smaller size of the heat sink will probably provide enough cooling rate to dissipate 70 W from the heat source.

4.2.2 Unit cell design

The model has been used to study the thermal design and evaluation technique for different unit cells, described earlier in Table 2. The temperature, pressure and velocity have been analysed and compared together with heat and mass flux aiming to identify the thermal performance established in three different possible unit cell of Cu-base heat sink, shown schematically in Fig. 2. The geometrical data for different cases are presented in Table 1. Computations were carried out using similar operating parameters. In addition, two different inlet conditions for constant inlet velocity (=2 m/s) and constant characteristic pressure drop (=25 Pa) have been compared for each case. Also flow behavior for turbulent and laminar condition have been studied. Further, to find out the best position of the fan for each case, the comparison of different inlet direction has been considered. Six different computations have been carried out for each case. To keep this report as short as possible, those results are not re-produced and only the basic features, needs for optimization issues, will be discussed here. The rest will be discussed in more detail in next section.

a) Case No. 1 (Rectangular heat sink based on straight fins)

Figure 15(a,b) shows typical results of velocity field and temperature distribution for case No. 1.

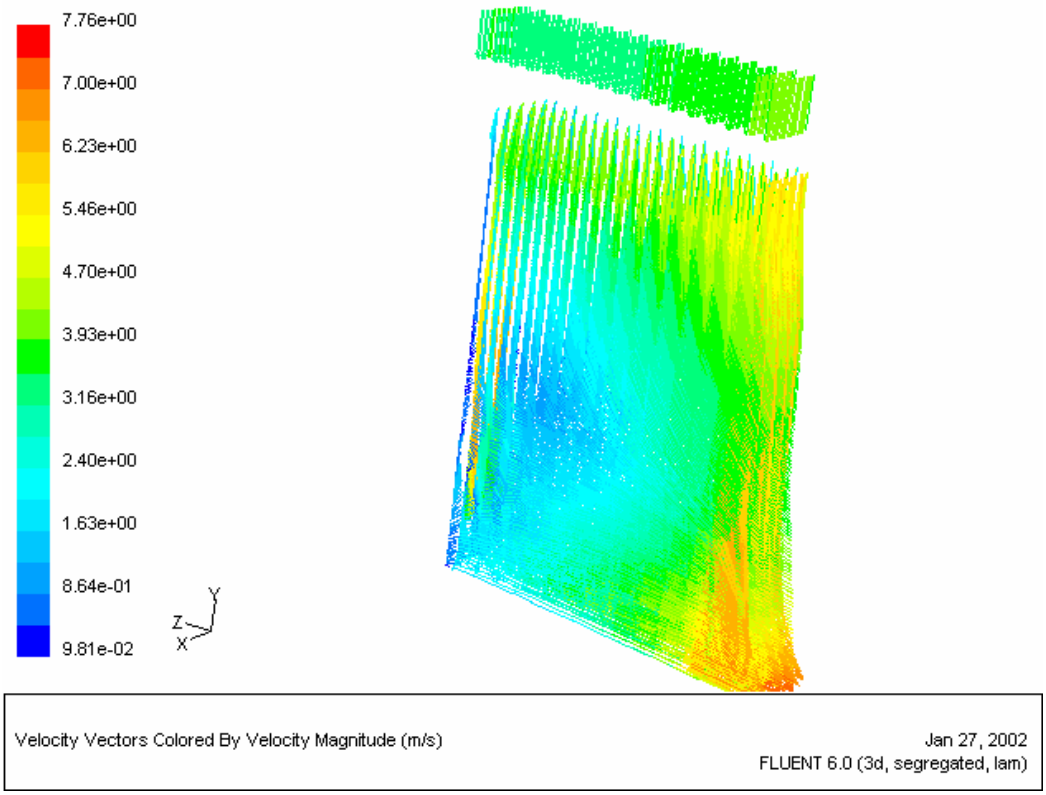

Fig. 15a) Velocity distribution in the unit cell

The figures show velocity vectors and temperature distribution in the entire unit cell, respectively. The results are comparable to those presented and discussed earlier through Fig. 9-14. In brief, it was observed that the velocity changes more intensely under the inlet fan from which the flow is withdrawn. It can also be seen that the temperature changes more intensely near the bottom plate (heat source) from where the heat is generated. This is common phenomenon for all different cases.

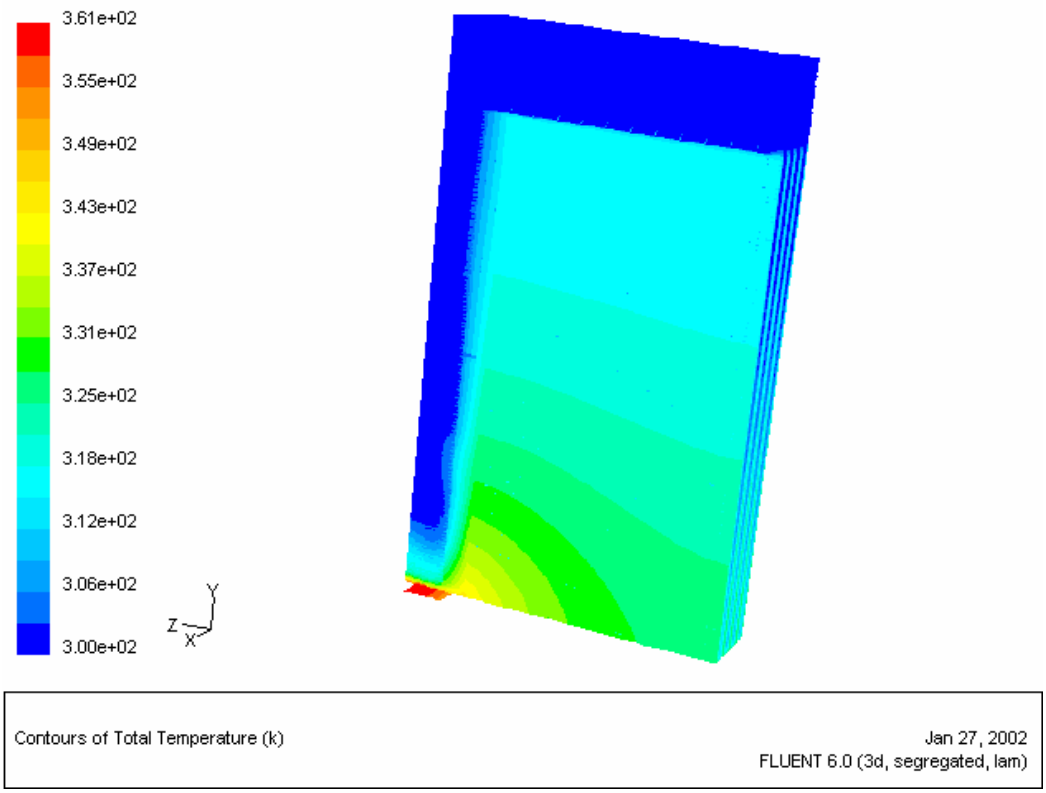

Fig. 15b) Temperature field in the unit cell

b) Case No. 2 (Rectangular heat sink based on triangle fins)

Comparing the temperature and velocity distributions for case No.2 shows a great dependency in relation with intaken fan position. Fig.16 shows the results when the fan is located on the top and Fig.17 shows the result with side located fan. It was also found that the flow behavior has great impact on the temperature, velocity and heat flux distribution in the heat sink unit cell, with a temperature difference around 63 K (375-312) when the side mounted fan is in used.

The results indicate that for highest efficiency of triangle-base heat sink, the flow has to pass through the fins; also a side-mounted fan will provide higher cooling effect. This will be discussed later. It also found that the three-dimensional model is needed for computation, in order to analyze the different design concepts.

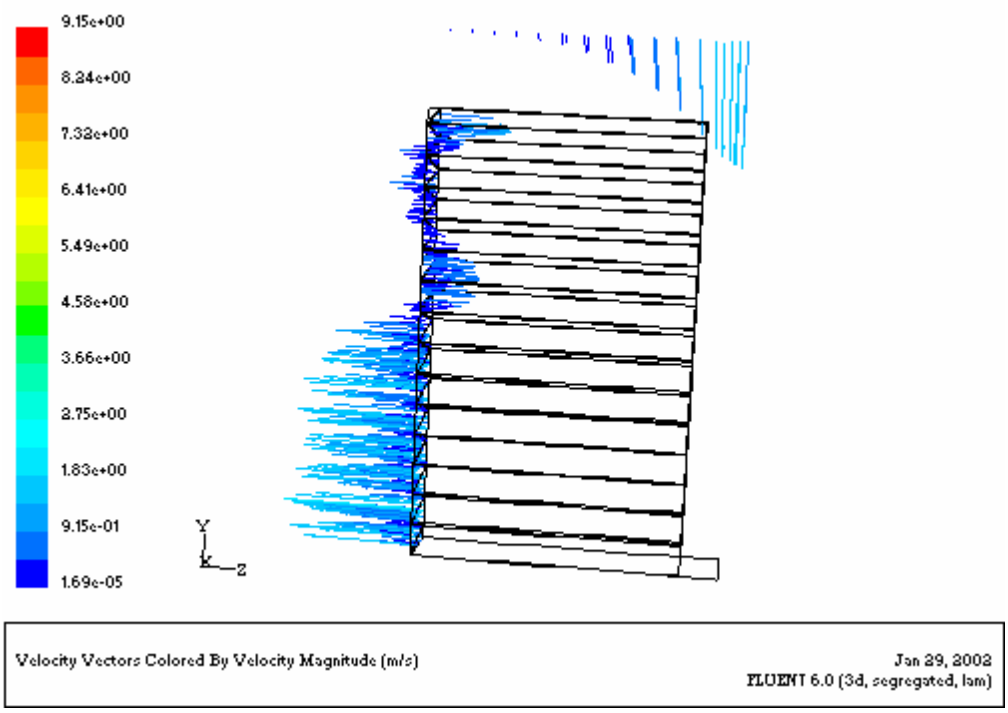

Fig. 16a) Velocity pattern in the unit cell with top mounted fan

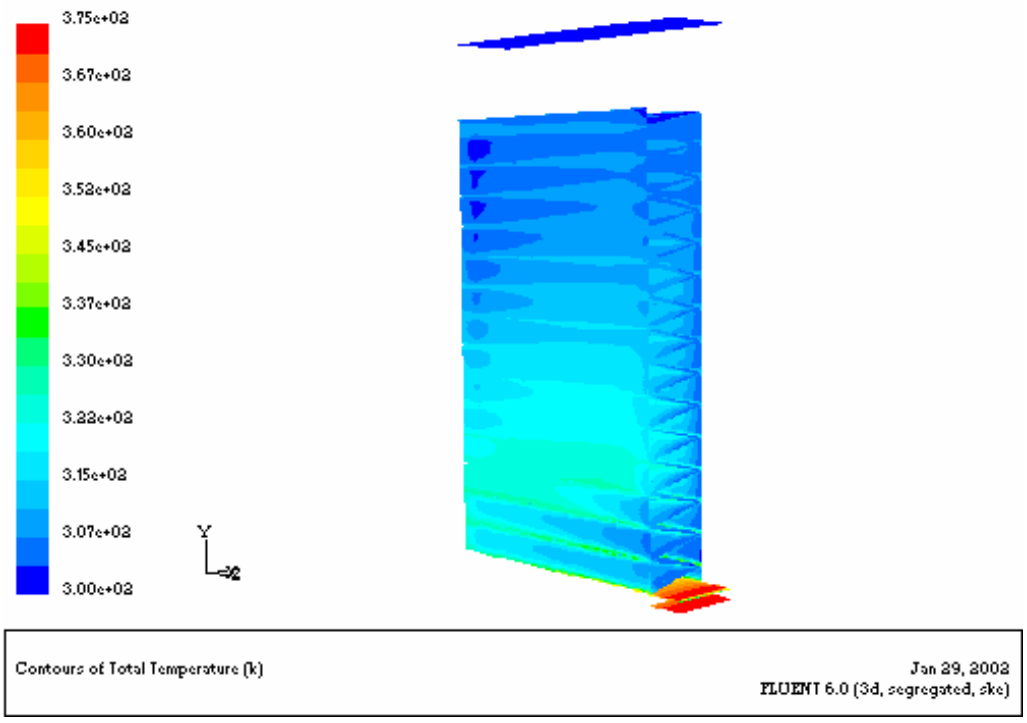

Fig. 16b) Temperature distribution in the unit cell with top mounted fan

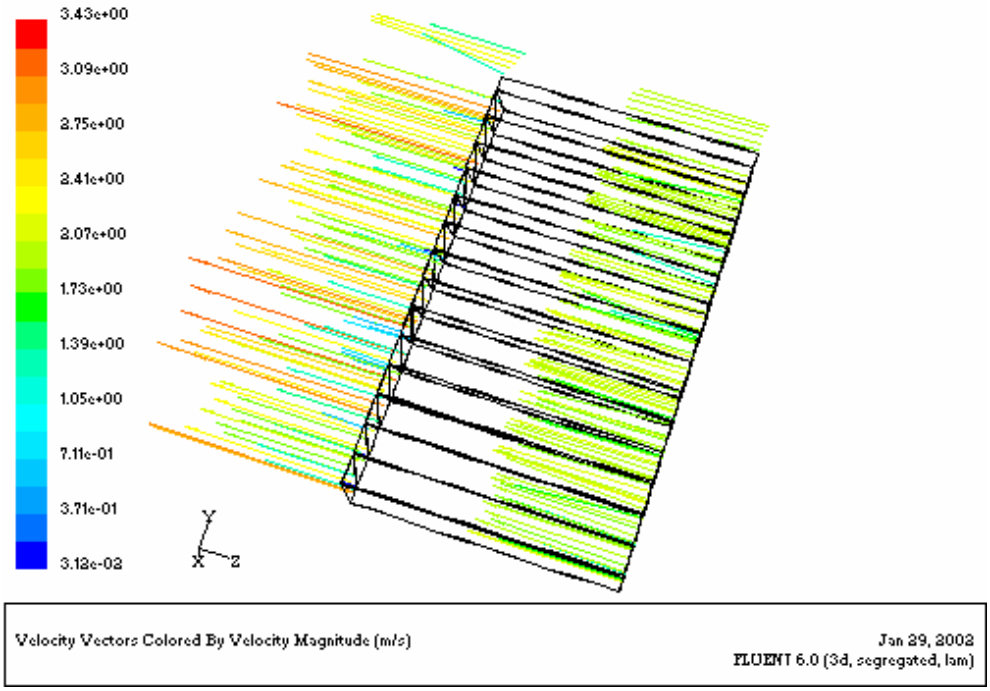

Fig. 17a) Velocity pattern in the unit cell with side-mounted fan

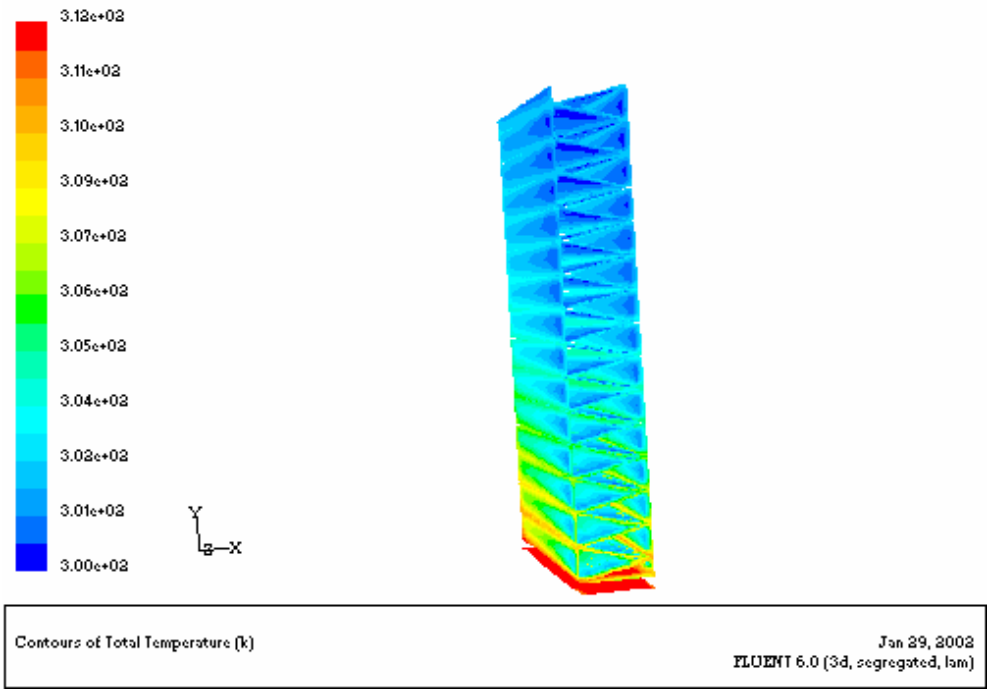

Fig. 17b) Temperature distribution in the unit cell with side-mounted fan

C) Case No.3 (Cylindrical heat sink based on triangle fins)

Figures 18 are typical of the results obtained for the velocity field and temperature distribution for case No. 3.

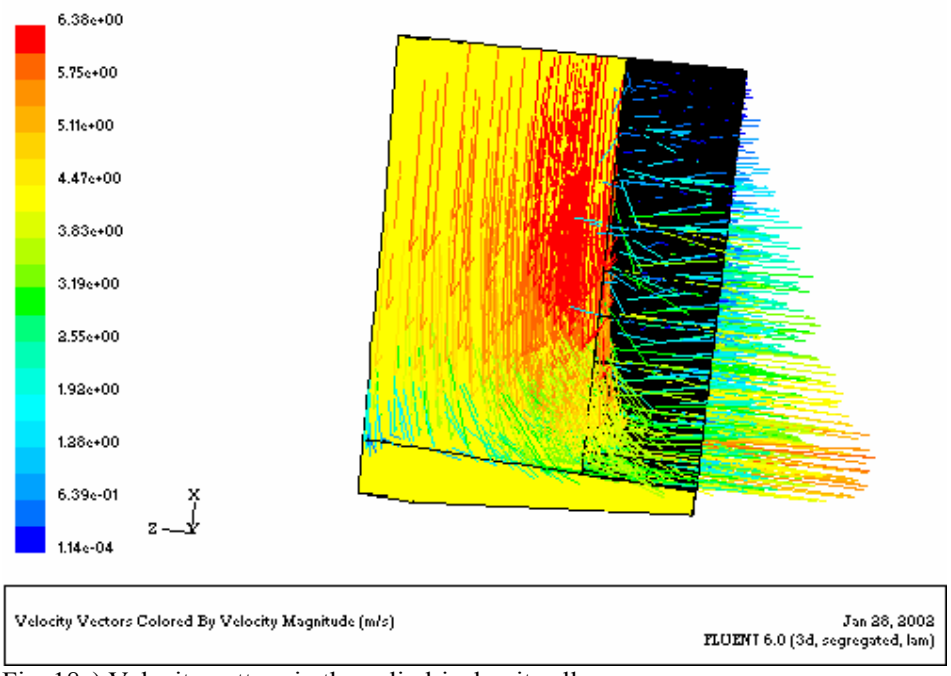

Fig. 18a) Velocity pattern in the cylindrical unit cell

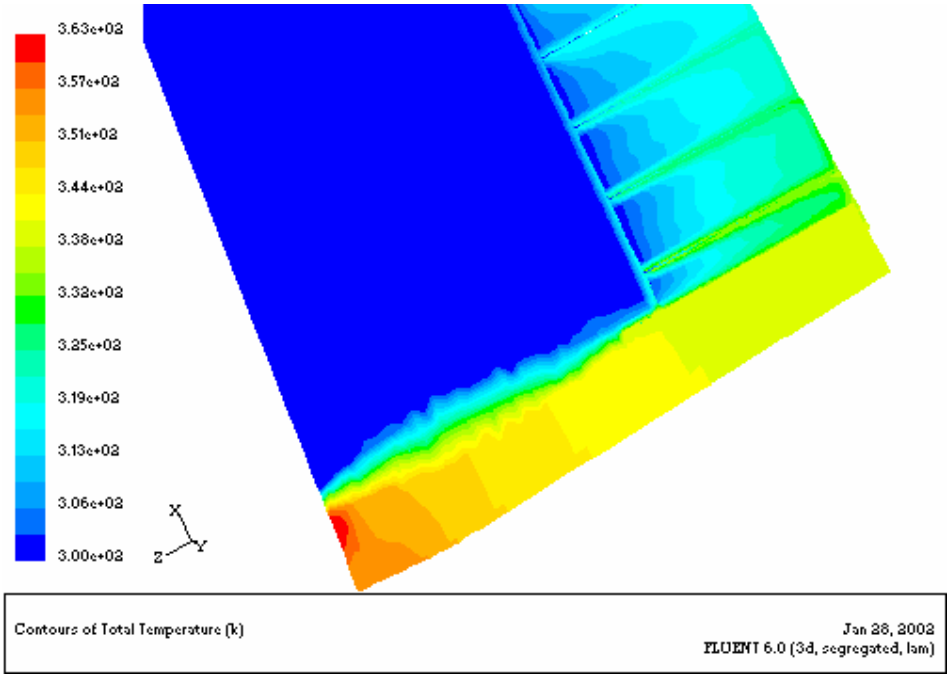

Fig. 18b) temperature in the cylindrical unit cell

The figures show velocity vectors and temperature distribution in the entire unit cell, respectively. The average velocity varies between 0.1 to 6.38 m/s when the maximum temperature around 363 K can be observed.

Comparing the results for different unit cells indicate that the pressure resistance for cylindrical geometry has its lowest value, and therefore, the highest inlet velocity will be produced in this case. The cooling process is controlled mainly by convection and therefore the contribution of the conduction is not significant, even though conduction has still major transfer method in releasing heat from the bottom plate.

To summarize, case No. 1 has highest efficiency in cooling process, in terms of convection and conduction contribution; when case No. 3 has the lowest efficiency in cooling process. Case No.2 is highly depended to the construction design in terms of inlet and outlet flow direction.

5. Optimisation & thermal performance

In order to optimize the overall heat sink, thermal performance should be maximized and weight satisfying constrains (dimension, manufacturing) should be minimized. The performance of a heat sink is measured by the temperature difference between heat sink base and the ambient air temperature. The objective of optimization is to minimize weight and volume of the heat sink and to meet temperature limitation for a given heat dissipation.
The model was also used to compare the performance of the six following heat sink designs:

- Aluminum in reference geometry
- Copper in reference geometry
- Case No. 1: Rectangular heat sink based on straight fins
- Case No. 2: Rectangular heat sink based on triangle fins
- Case No. 3: Cylindrical heat sink based on triangle fins
- Case No. 4: Rectangular heat sink based on straight thin fins

The numerical results are presented first. The optimization issues and the comparison of the thermal performance for different cases will be described following the presentation of the numerical results.

5.1 Case No. 1: Rectangular heat sink based on straight fins

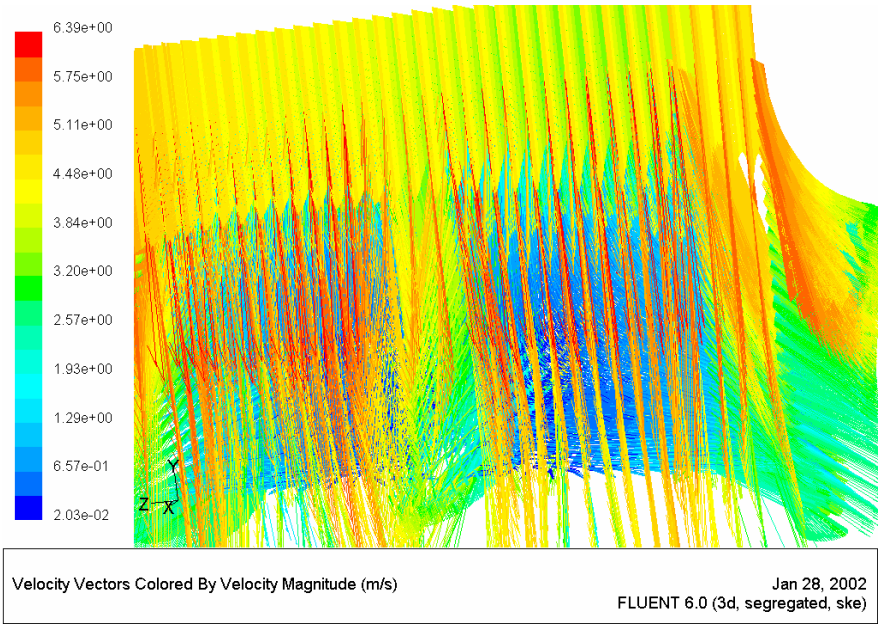

Fig. 19a) Velocity pattern in the domain

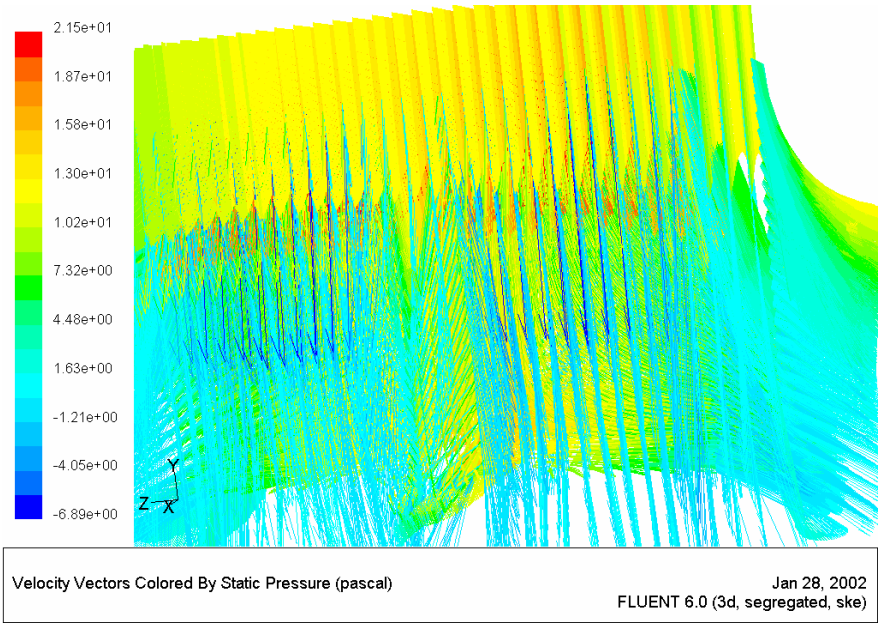

Fig. 19b) Pressure pattern in the domain

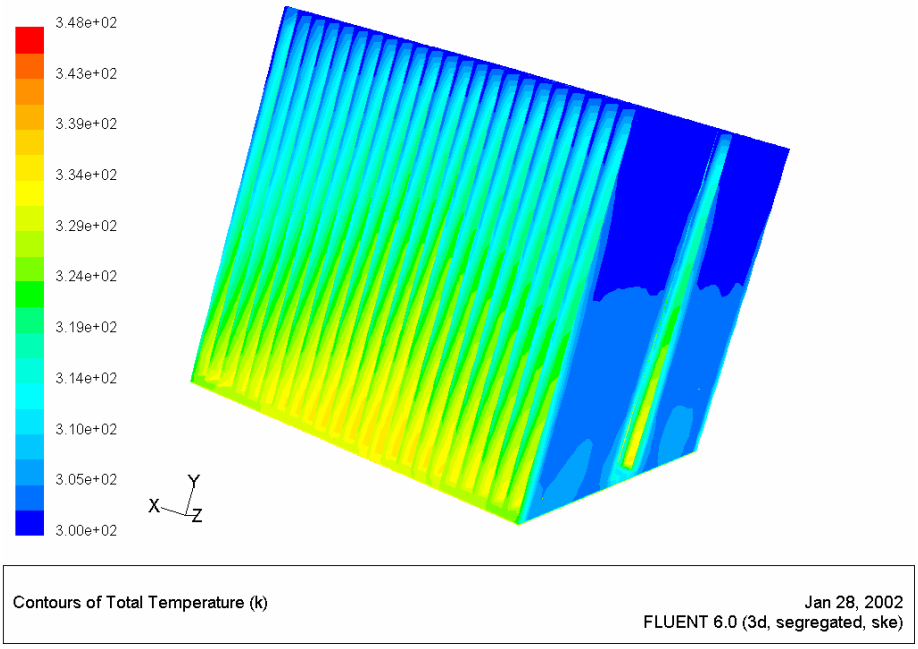

Fig. 19c) Temperature distribution in the domain

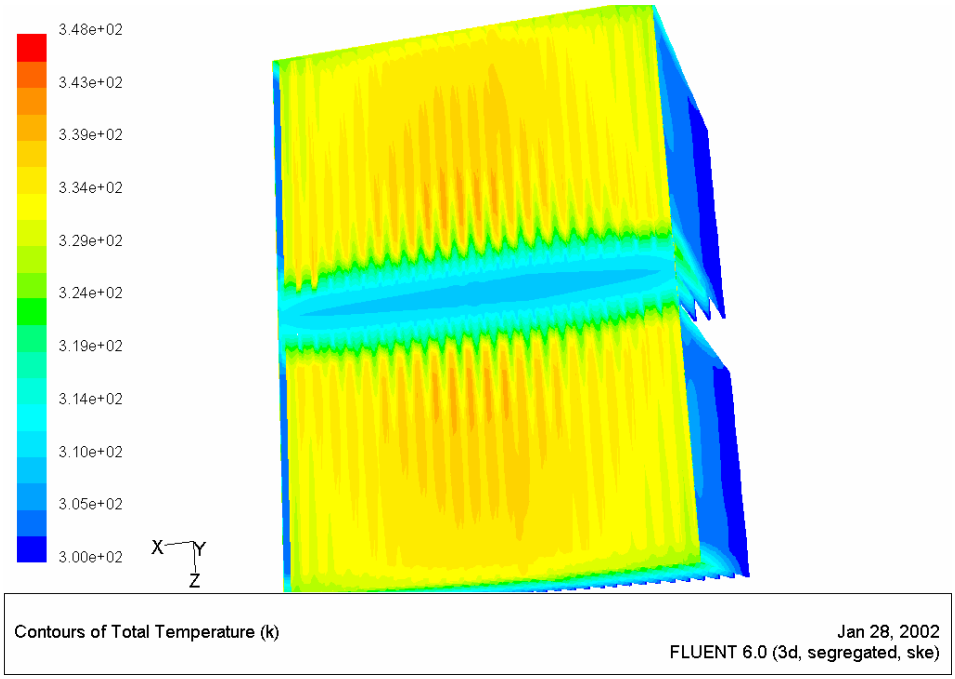

Fig. 19c) Temperature distribution in the domain

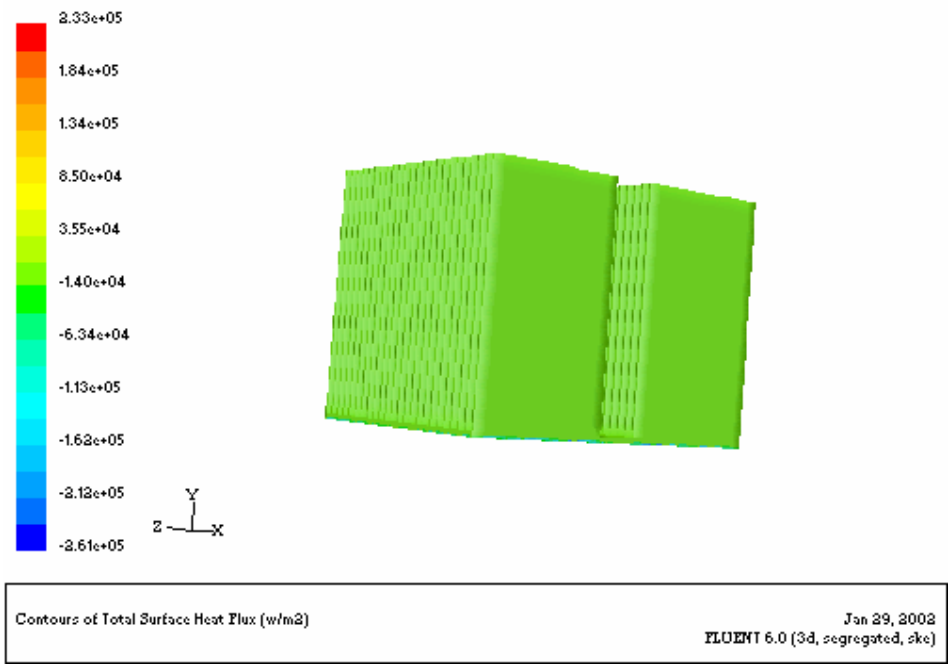

Fig. 19d) Heat transfer coefficient pattern in the domain

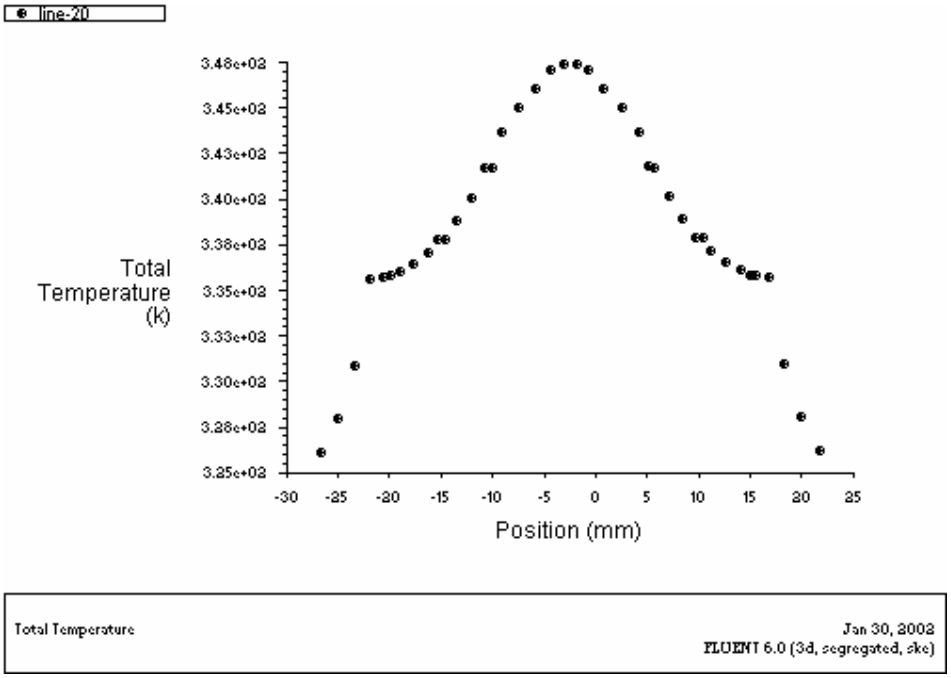

Fig. 19d) Temperature distribution in the bottom plate

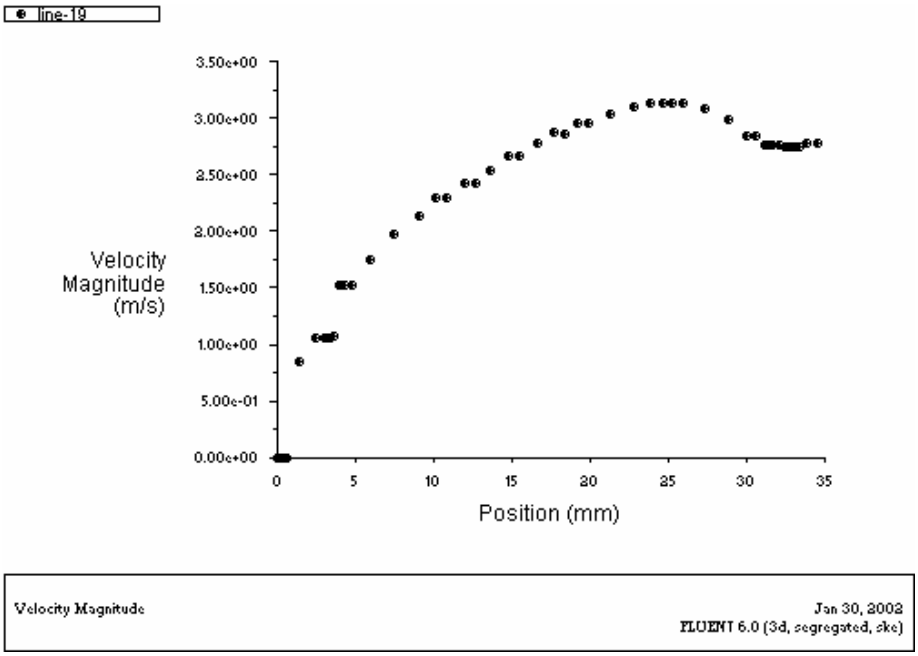

Fig. 19d) Velocity distribution in the longitudinal direction

5.2 Case No. 2: Rectangular heat sink based on triangle fins

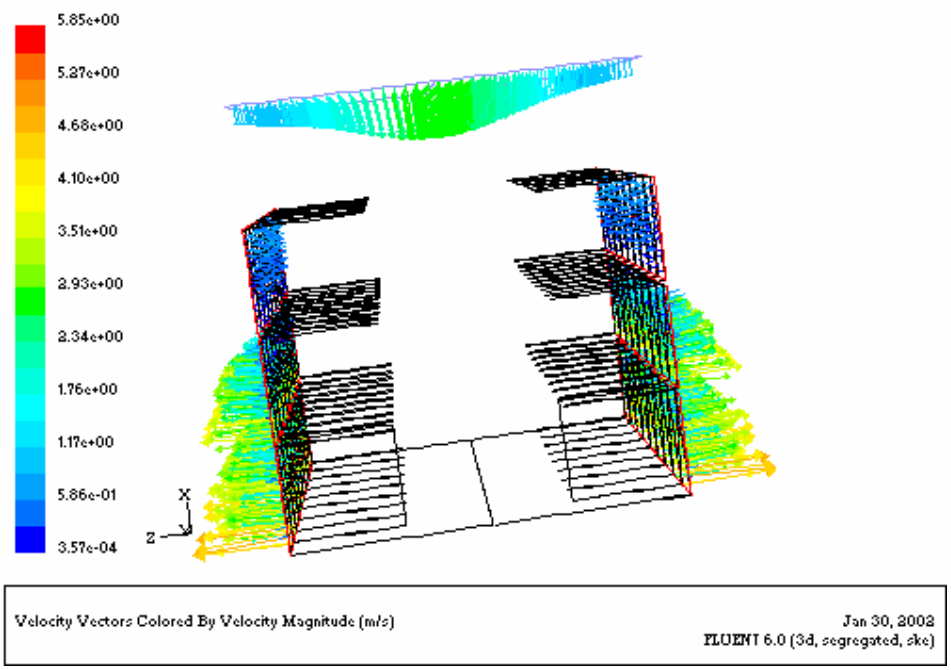

Fig. 20a) Velocity pattern in the top mounted fan

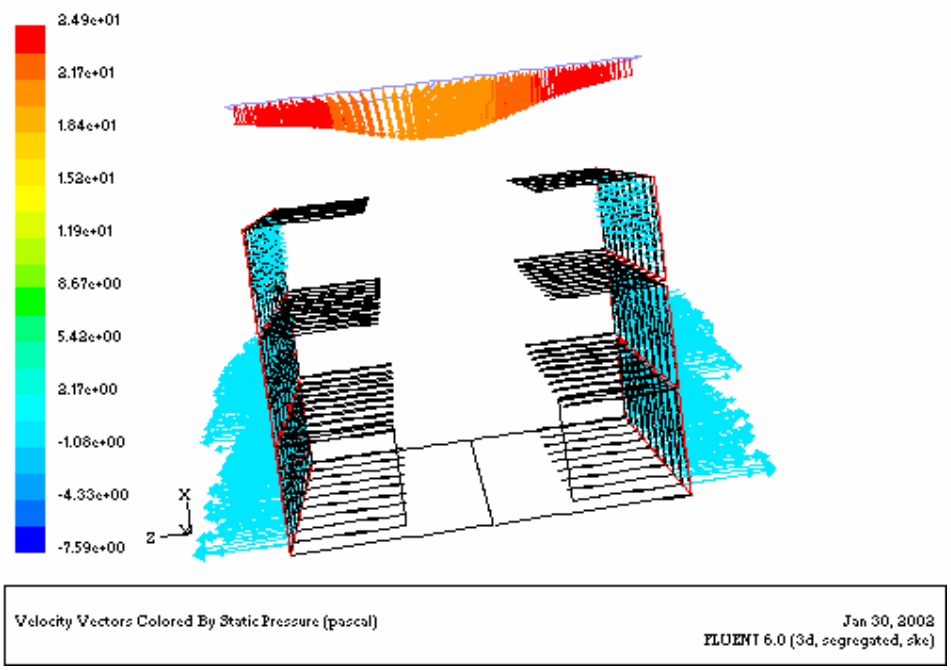

Fig. 20b) Pressure pattern in the top mounted fan

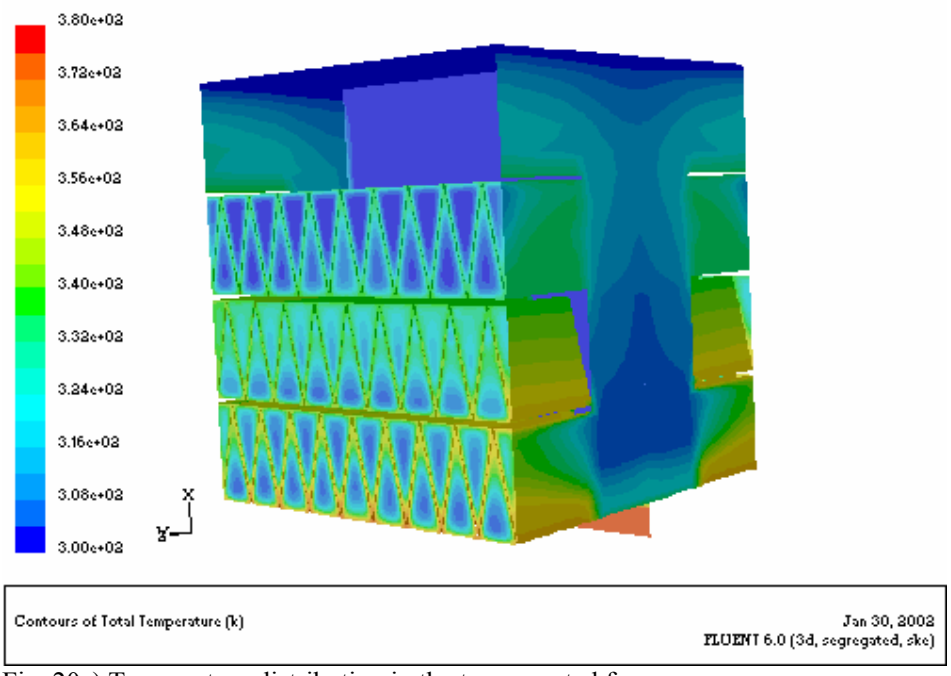

Fig. 20c) Temperature distribution in the top mounted fan

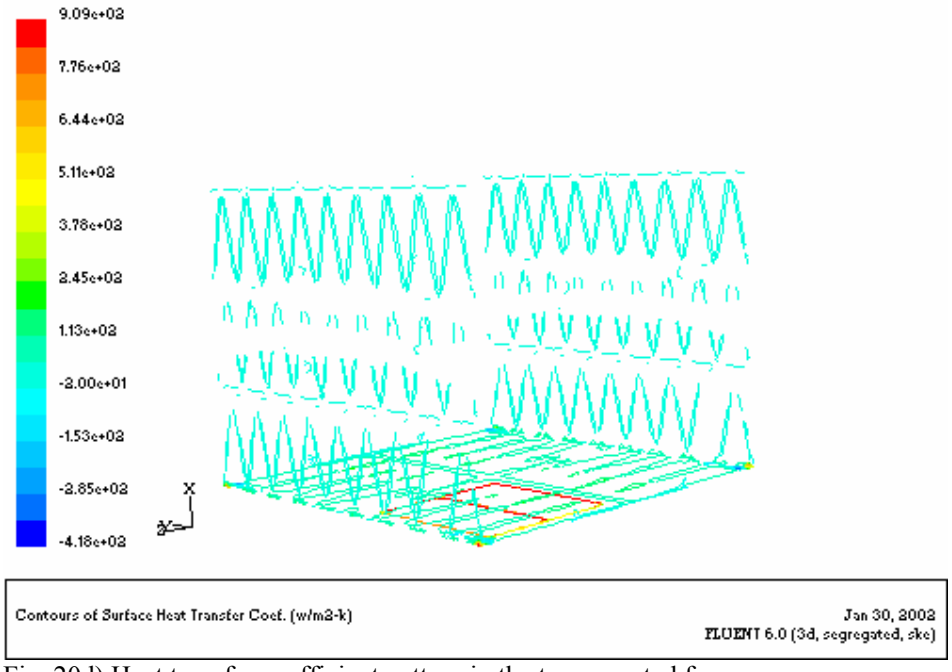

Fig. 20d) Heat transfer coefficient pattern in the top mounted fan

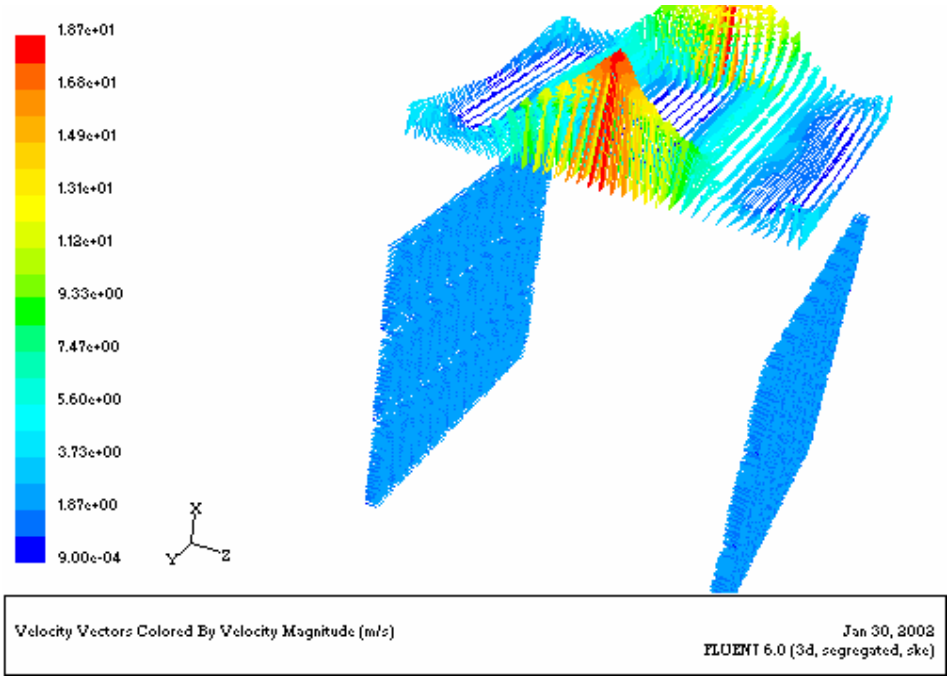

Fig. 21a) Velocity pattern in a top mounted suction mode fan

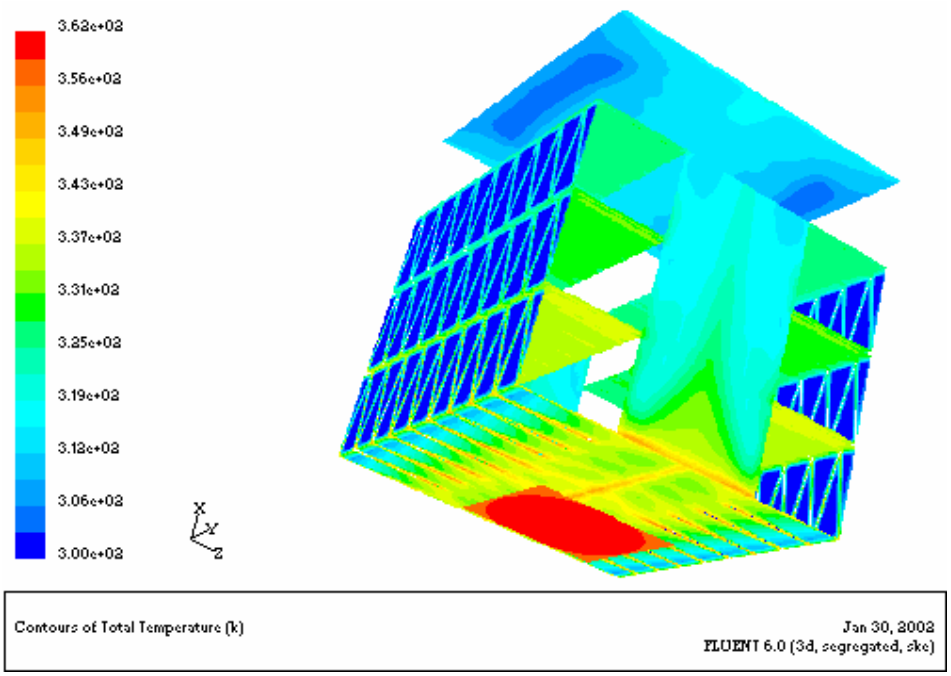

Fig. 21b) Temperature distribution in a top mounted suction mode fan

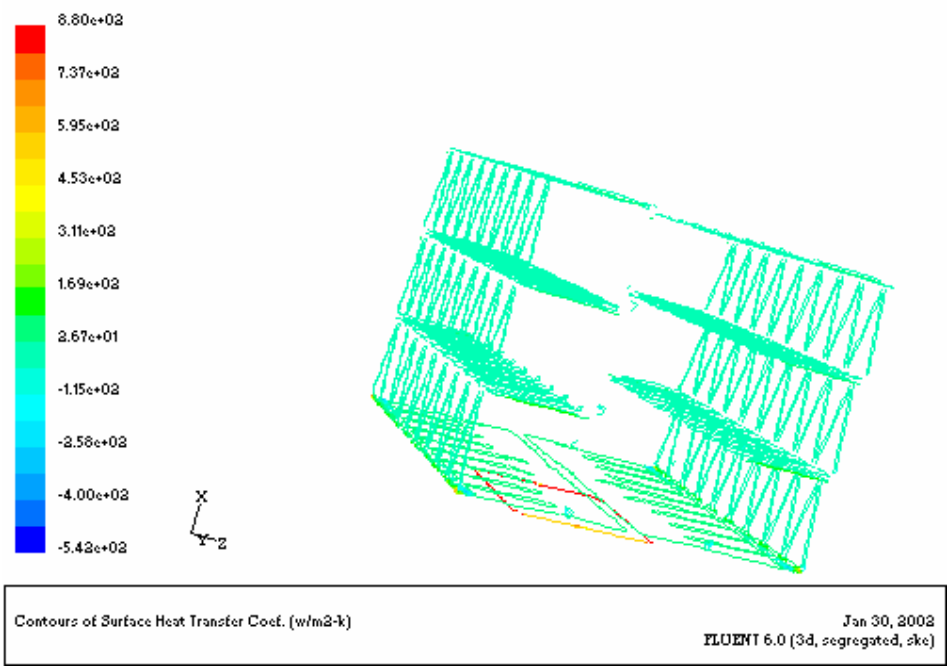

Fig. 21c) Heat transfer coefficient in a top mounted suction mode fan

5.3 Case No. 3: Cylindrical heat sink based on triangle fins

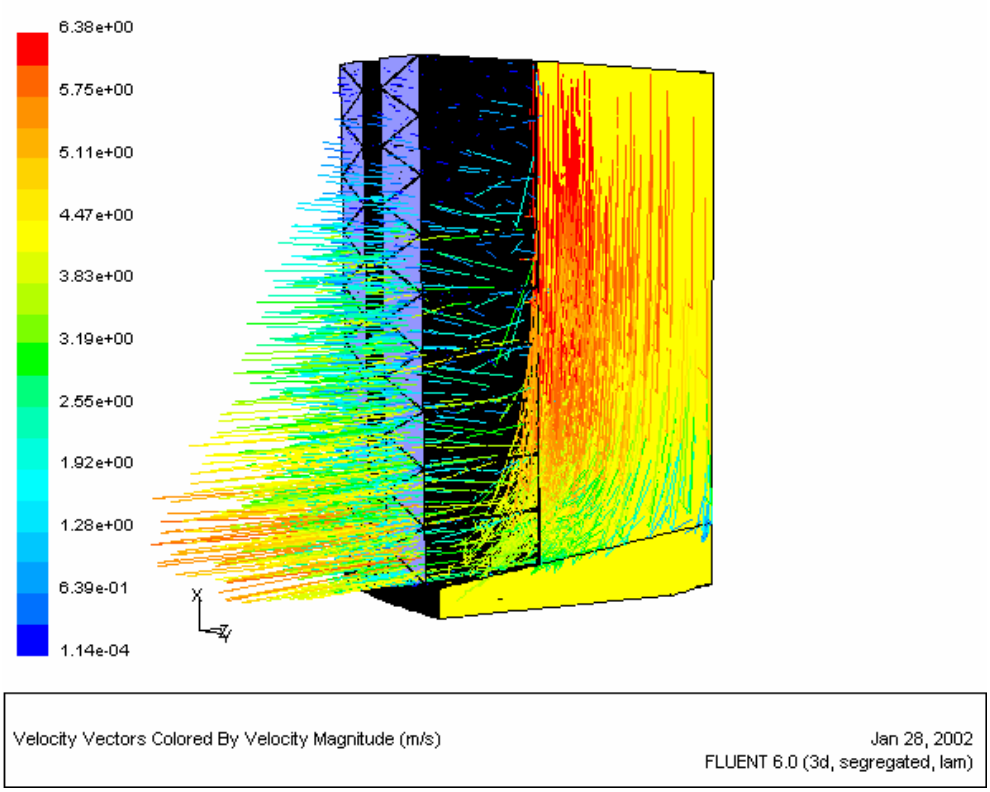

Fig. 22a) Velocity pattern in the domain

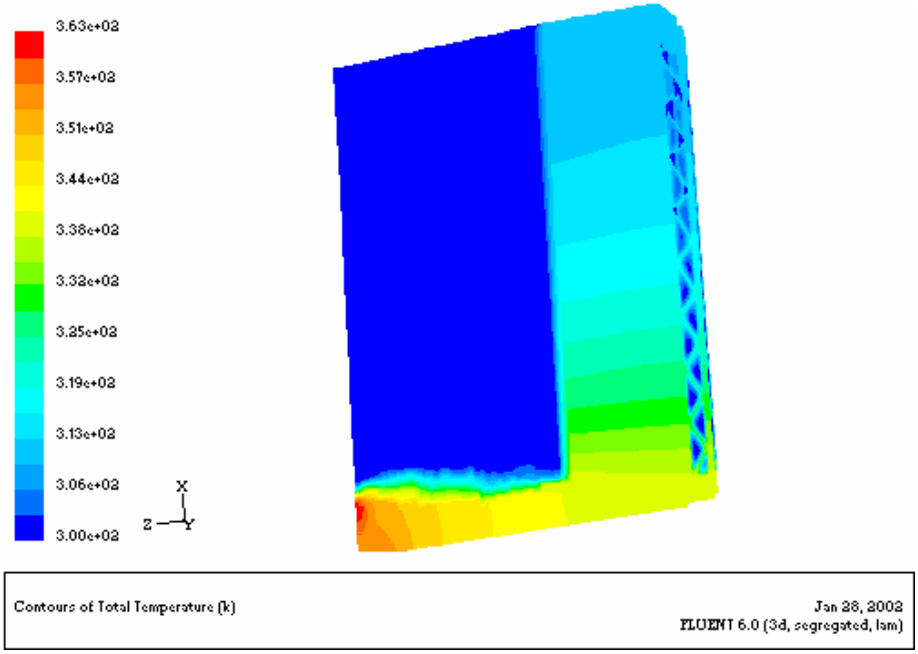

Fig. 22b) Temperature distribution in the domain

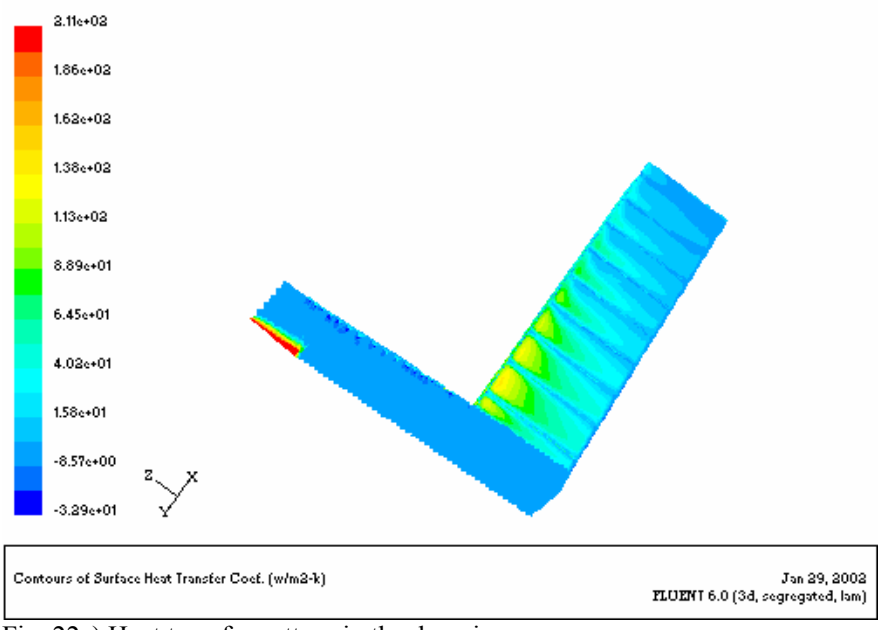

Fig. 22c) Heat transfer pattern in the domain

5.4 Case No. 4: Rectangular heat sink based on straight thin fins

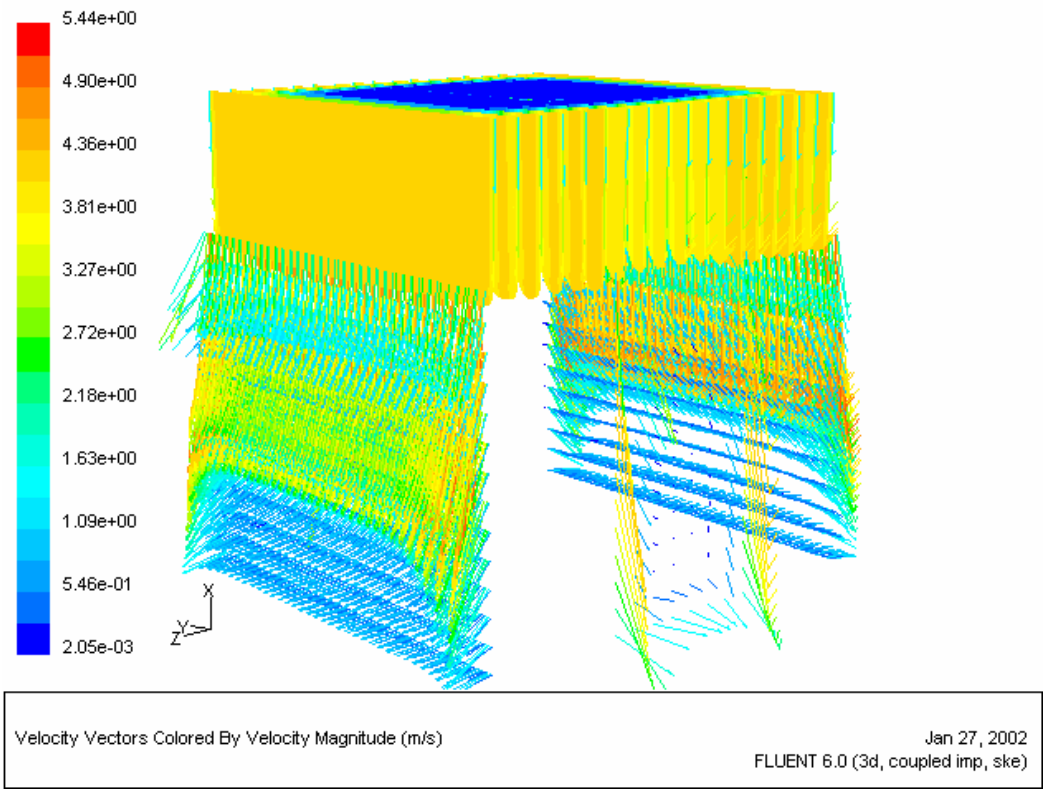

Fig. 23a) Velocity pattern in the domain

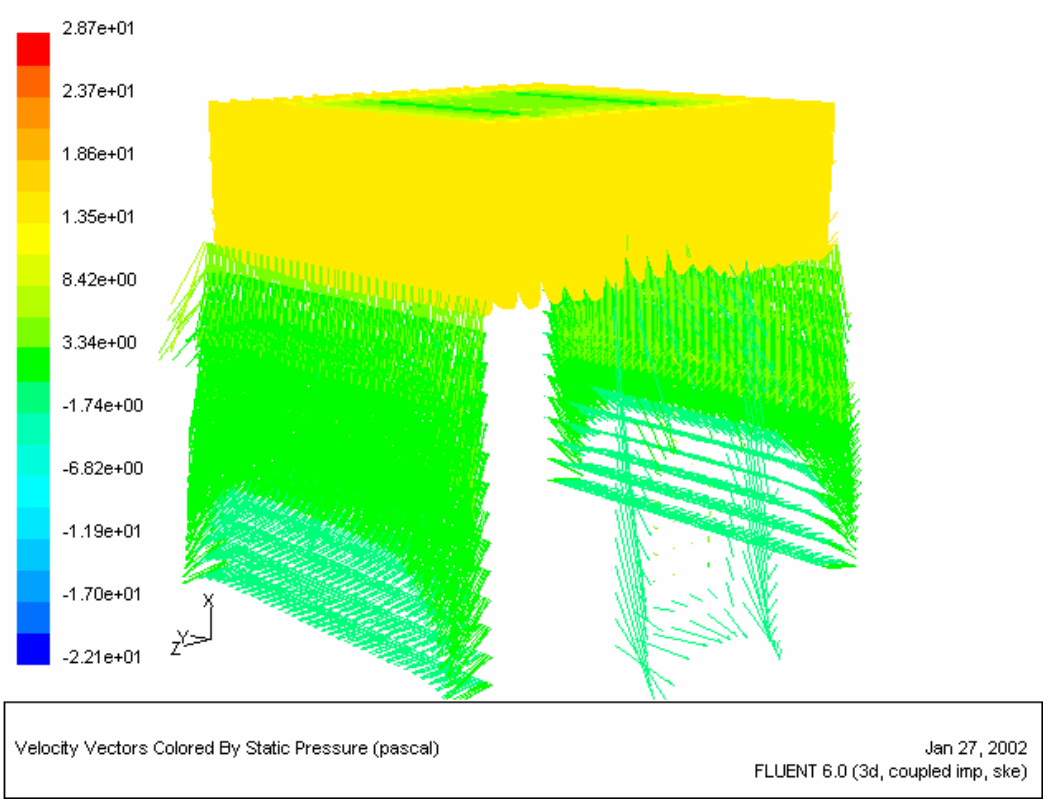

Fig. 23b) Pressure distribution in the domain

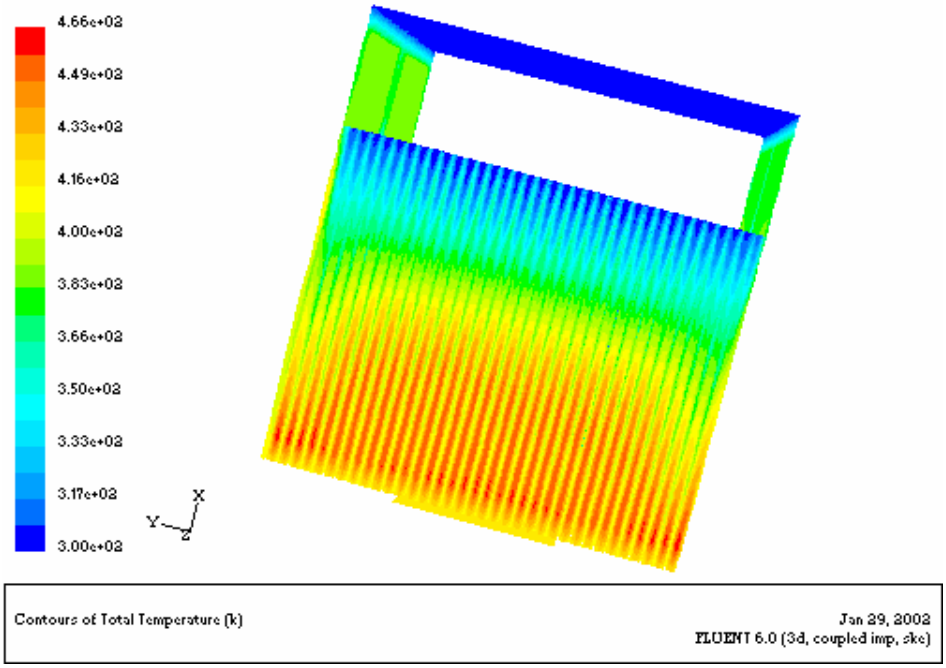

Fig. 23c) Temperature distribution in the domain

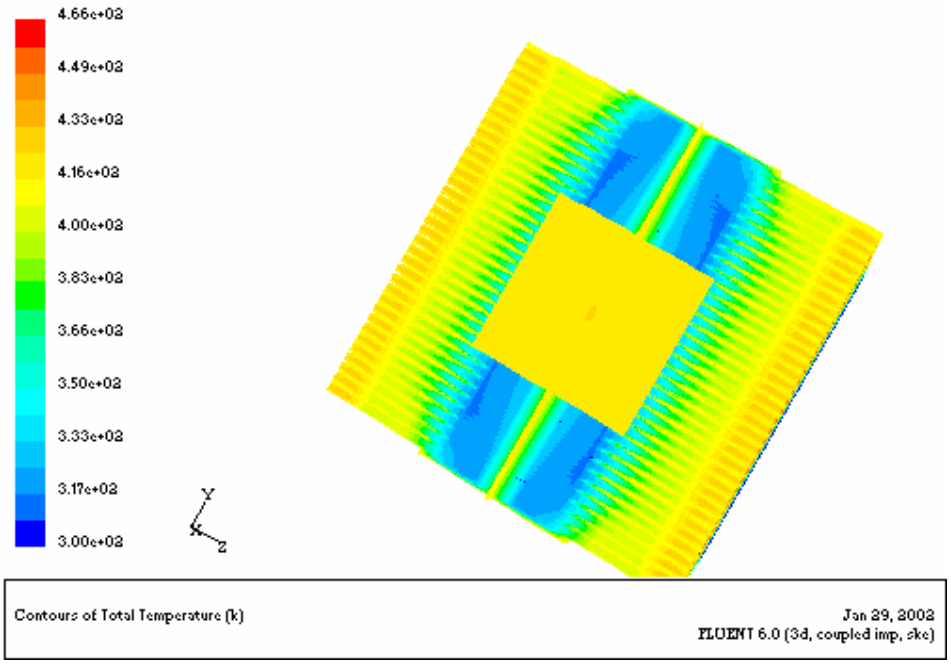

Fig .23d) Temperature distribution in the domain

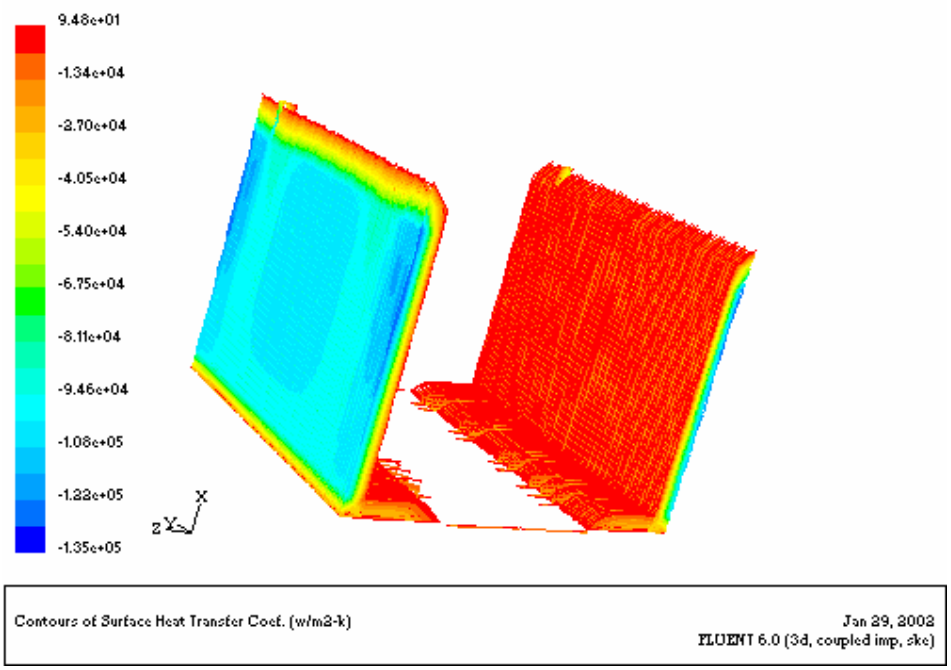

Fig. 23E) Temperature distribution in the domain

Table 3: Computation results

Case simulated	Q_{in}	ΔP_{in}	$\bar{V}_{inlet}$	$\dot{m}$	T_{max}	V_{max}	ΔP_{max}	$\bar{h}$	$h_{heatsour}$	***Mass flow rate***	***Weight***
Unit	*W*	*Pa*	*m/s*	*kg/s*	*K*	*m/s*	*Pa*	W/m^2K	W/m^2K	*(Kg/s)(m/s)*	*g*
Rf_Al	70	25	4.4	0.037	341	6.9	23.6	49	229	0.1617	159
RF_Cu	70	25	4.4	0.037	325	6.9	23.7	52	3605	0.1617	531
Case 1	70	25	3.27	0.0008	348	6.3	21.5	147	8122	0.029	97
Case 2 1/2	35	25	1.24	0.0012 0.0024	380/60	5.58	25	57	909	0.0028	76
Case 3 1/25	2.8 x25	25	6.2	0.0003	363	6.3	27.8	68	14105	0.002	116
Case 4 1/2	38	25	1.63	0.001 0.0019	466	5.44	28.7	77	2349	0.0032	66

Case1	**Case2**	**Case3**	**Case4**
30 x 25 x 40	35*35*30	D=60, l=30, t=10	35x35x30

It has been tried to summarize the computation results in Table 3, to get some insights for comparing the thermal performance and be able to address optimizing issues. It proves convenient for the purpose of grid generation (repining the nodes number in a reasonable manner, as well as ending up with less difficulties) to discretise:

- the whole geometries in Cases Rf_Al, Rf_Cu and No. 1;
- half of the geometry in Cases 2 and 3 (symmetric geometry)
- and only discretise 1/25 of the geometry in Case No.4 (Asymmetric geometry);

even though, these may cause problems in comparing the results directly.

The first and second columns in Tables 3 show the boundary conditions used in this computation. The computed average inlet velocity, mass flux and mass rate flow based on continuity equation are shown in columns 3, 4 and 10 when the maximum *h* at the heat source area of the bottom plate are given in column 9 in the table. Columns 5-8 indirectly summarize the results given in Fig. 19a up to 23e for different cases, which the accuracy of those average values could be argued. Finally, the calculated weight and dimension are also given.
The local heat and mass fluxes are the greatest in the inlet portion of the heat sink for all cases and they are decreased rapidly in the longitudinal direction. The distributions of the local heat fluxes are presented at the inner walls of the fins, where the solid and fluid are in direct contact. The heat fluxes are taken to be positive if they are directed from the solid to the fluid, and negative, otherwise. Furthermore, the modified mass flow rate (m/s)(kg/s) is used to compare different design concept.
Predictions of the thermal parameters from simulations are within acceptable limit compared to those reported earlier. Note that the heat sink maximum temperature hardly can be measured.
The close correlation between modelling and measurements give good confidence that other heat sink structures can be modelled without need for confirmation testing. The ability to use computational fluid dynamics to define the performance of a heat sink and to optimize a heat sink provides cost and time saving in testing, equipment used in testing and finallytest resources.

Back to the table; the following important observations can be deduced:

- Comparing the calculated weight and dimension with the reference case Ref_Al, show that the weight constrains have been satisfied in all cases, even though cylindrical geometry (case No. 3) is bigger than the others;
- Comparing the average inlet velocity together with mass flow rate/ mass flux at the inlet area, one could conclude that the cylindrical case has lowest pressure resistance when case 2 and 4 have the highest;
- Case 3 does not show very high efficiency due to relatively low contribution of conduction in this case (T_{max}=363K). It has been discussed earlier that the cooling process in this case is controlled by mainly air flow, blowing directly against the rather big open area in the central region (D=40 mm) of the heat sink. In brief, fins do not have considerable effect in the cooling process in this case.
- Case No.2 is highly depended to the inlet/outlet direction, which shows more efficient when the air can pass through all fins by using suction or side mounted fan design. (T_{max}=380 against 362 K). This means, however, with a suitable design, this could be efficient enough to be considered as a next generation heat sink. The modelling work can be used to provide insight into the details of the air flow path in and around the heat sink. There are some very narrow clearances that make it difficult for the approach air flow to significant portions of the heat sink. A new design with larger clearances avoids this problem and has markedly better performance. However, more research work is needed to find the most suitable construction design.
- Theoretical analysis suggest that *Rectangular heat sink based on straight fins* case No.1 has a superior potential for application in thermal management of the electronic packages. This design is compact enough, light enough and also is capable of dissipating a significant thermal load (heat transfer coefficient of order 147 W/m^2 K) with a relatively small increase in the package temperature (less than 50 K), if operated with a thickness above 3.5 mm; it is worth to note:
    - i) The thickness of the copper base-plate was varied between 1 to 5 mm to find out the optimum thickness for the bottom plate. It was found that a thickness around 3.5-4 mm seems to be an optimum thickness i.e. increasing the thickness of the bottom plate more than 4 mm has no additional direct effect on the heat spreading in the heat sink. More experimental and theoretical research works in this issue are recommended.
    - ii) The model was used to analyse the possibility of using thinner and more close packed fins (from t = 0.25 mm x 24 to 0.1 mm x 70 in Case No. 4).

It was found that there is limitation in using thinner fins; since as the number of the fins increased (and the thickness has been decreased) the pressure resistance through the fin region will increase with a negative effect on the inlet velocity and mass flow rate. The maximum temperature in the domain will also increase which means that there will be some limitation in decreasing the fins thickness.

iii) In the analysis of the overall thermal performance of the heat sink, one should also note that the maximum increase in operating temperature does not exceed 80 K, while quite large heat fluxes of 70 W were successfully dissipated.

iv) Finally the results confirm that a rather high average heat transfer coefficient (in order of 120-170 W/M^2 K) can be achieved in the straight fin base copper heat sink.

- Large temperature gradients near the air inlet are likely to induce significant thermal stresses and, therefore, must be carefully considered in the practical heat sink design in order to avoid mechanical failure.

6. Remarks and suggestion

The theoretical analysis performed, provides a fundamental understanding of the combined flow and conjugate convection-conduction heat transfer in the copper-base heat sink. The developed three-dimensional mathematical model, using incompressible turbulent Navier-Stokes equations of motion, is capable of predicting correctly the flow, temperature and heat distribution in the domin. It has been validated using available data-reported earlier.
This work, however, represents a critical first step toward a systematic approach to the design of Cu-base heat sink, for improvement of the productivity and quality of the cooling process in electronic device. The thermal performance of different proposed constructions are modelled and studied numerically. In particular, this study is focused on the temperature distribution, the thermal resistance and the optimization of geometrical design parameters. The present work establishes the process for a tailored design and optimization of a Cu-base heat sink. Our result demonstrates that a rectangular heat sink based on the straight fins can be considered as a substantial improvement over a conventional Al-base heat sink. Further, it was found that the rectangular Cu-base heat sink with triangle fins could also be considered as an alternative.

Additional work must be done, however, before this goal can be achieved. Several additional phenomena remain to be investigated in the air inlet system, including:

- thermal resistance between the heat source and bottom plate,
- thermal resistance between fins and holder metal,
- different inlet/outlet location,
- implementing rotating fan instead of normal to the inlet surface,
- further modification in the geometrical heat sink design including
    - thickness and number of the fins (fin pitch),
    - fin geometry (plate, rod and etc.)
    - thickness of the bottom plate
    - dimension optimization

This work presents many challenges for future mathematical models. This new concept, presented here, must be interpreted, with the help of *experimental studies*, to quantify how it behaves.

Acknowledgements

The authors are grateful to Dr. Leon Tang and Msc. Per Sandberg for many fruitful discussions, ideas and help regarding this work.

References

1. Vafai, K and Zhu, L.; *Heat and Mass Trans.*; 42 (1999) 2287-2297.
2. T.Y.Chang, *et al*., *J. of Electronic Packaging* Vol. 123 (2001) 225-230.
3. S. Gu, T.J.Lu and A.G. Evans, *Int. J. heat mass transfer*, V. 44 (2001) 2163-75.
4. Zhang, H.Y and X.Y. huang, *Int. J. heat mass transfer*, V. 44 (2001) 1593-1603.
5. Vladimir V *et al*, *Int. J. heat mass transfer*, V. 43 (2000) 3481-3496.
6. Maveety J.G and H.H Jung, *Int. Comm. Heat transfer*, V. 27 (2000), 229-240.
7. Mustafizur Rahman, M, Int. Comm. Heat Mass Trans., V. 27 No. 4 (2000), 495-506.
8. Kim, S.J. *et al* , *Int. J. heat mass transfer*, V. 43 (2000) 1735-48.
9. Morega, A. *et al*, *Int. J. heat mass transfer*, V. 38, No. 3 (1995) 519-531.
10. Lu, T.J, *Int. J. heat mass transfer*, V. 42 (1999) 2031-40.
11. Lage, J.L *et al*, *Int. J. heat mass transfer*, V. 39, No. 17 (1996) 3633-47.
12. Ledezam, G and A. Bejan, *Int. J. heat mass transfer*, V. 39, No. 9 (1996) 1773-83.
13. Bhavani, S, *IEE Trans;* 24 (2001) 166-175.
14. Shin, Donglyoul; Tech. Report; *Samsung Electronic Co; Flowtherm Web side*
15. Fedorov, A.G. and Viskanta, R; *Heat and Mass Trans.*; 43 (2000) 399-415
16. Sabri, M. N; Tech. Rrans. Of the ASME; 123 (2001) 344-350.
17. Kevin, G ; Tech. Report; *Thermacore, Inc; Flowtherm Web side*
18. Sabry, M.N*; IEE Trans;* 23(2000 562-567
19. Biber, C; Tech. Report; *Wakefield Eng.; Flowtherm Web side*
20. Behm, J; and Huttunen, J; *Int. Flowther user Con*.,2001
21. *Grubb, K..;* Tech. Report, *Thermacore, Inc*, www. Thermacore.com.
22. *Fluent user guides, Fluent6, 2001.*